SHEAR STRENGTH OF PRECAST, PRESTRESSED STEEL FIBER REINFORCED CONCRETE HOLLOW-CORE SLABS

by

Gustavo J. Parra-Montesinos
Luis B. Fargier-Gabaldón
Mohamed Al-Tameemi

University of Wisconsin-Madison
Department of Civil and Environmental Engineering

November 2019

TABLE OF CONTENTS

LIST OF TABLES

LIST OF FIGURES

ACKNOWLEDGEMENTS

SUMMARY

Precast, prestressed concrete hollow-core slabs are commonly used in residential, office and industrial construction because of their light weight, rapid construction, and large span-to-depth ratios. These structural members are typically manufactured using either an extrusion (e.g., Elematic) or a slip-form process. Although most hollow-core slabs have depths not exceeding 12 in. (305 mm), there are cases in which deeper slabs are needed to satisfy strength and serviceability requirements. Results from past research (Hawkins and Ghosh, 2006), however, have indicated that deep hollow-core slabs may fail at shear forces substantially lower than the web-cracking shear strength, V_{cw}, calculated according to the ACI Building Code. Because of this, ACI 318-14 limits the shear strength of hollow-core slabs with overall thickness greater than 12.5 in. (320 mm) to half of the web-cracking shear strength, unless at least minimum shear reinforcement is provided.

In this research, the use of randomly oriented, deformed steel fibers in hollow-core slabs was evaluated as minimum shear reinforcement in extruded and slip-formed prestressed concrete hollow-core slabs. A total of 14 and 16 tests were conducted on extruded and slip-formed hollow-core slabs, respectively. For the extruded slabs, the shear span-to-effective depth ratio was either 3.0 or 3.5. For the slip-formed slabs, on the other hand, the shear span-to-effective depth ratio ranged between 2.0 and 3.0. Two types of hooked steel fibers were evaluated. Type 1 fibers were 1.18 in. (30 mm) long, 0.022 in. (0.55 mm) in diameter, and had a specified tensile strength of 160 ksi (1100 MPa). Type 2 fibers, on the other hand, were 2.36 in. (60 mm) long and 0.035 in. (0.9 mm) in diameter, with double hooks at each end. The nominal tensile strength for the Type 2 fibers was 335 ksi (2300 MPa). In the extruded slabs, Type 1 fibers were evaluated at 50 lbs/yd^3 or 290 N/m^3 (0.38% volume fraction), while Type 2 fibers were evaluated at 40, 50 and 62 lbs/yd^3 (230, 290 and 360 N/m^3) for fiber volume fractions of 0.30, 0.38 and 0.47%, respectively. In the slabs constructed using a slip-form process, Type 1 fibers were evaluated at 55 and 66 lbs/yd^3 (320 and 385 N/m^3), which corresponded to a fiber volume fraction of 0.42 and 0.50%, respectively, while Type 2 fibers were evaluated at 40 and 50 lbs/yd^3 (230 and 290 N/m^3), which corresponded to a fiber volume fraction of 0.30 and 0.38%, respectively.

Extruded hollow-core slabs with Type 1 and Type 2 fibers in volume fractions of up to 0.38% (50 lbs/yd^3 or 290 N/m^3) could be mixed without any changes to the original mixture proportions or mixing process. From observations during manufacturing of the slabs and the test results, it appears that some difficulties in terms of mixing and fiber distribution could be encountered when using Type 2 fibers in a 0.50% volume fraction. Manufacturing of slip-formed hollow-core slabs, on the other hand, proved challenging when using Type 2 fibers, particularly in volume fractions of 0.38%. In some instances, manufacturing of these slabs had to be paused to clear fibers trapped in the slip-form machine. On the other hand, no major difficulties were encountered in the manufacturing of slabs with Type 1 fibers at dosages of up to 0.50% by volume.

Strand end slip values in the slabs constructed using an extrusion method did not seem to be affected by the presence of fibers. Fifty strand diameters ($50d_b$) represented an adequate, and generally conservative estimation of the average transfer length for 0.6 in. diameter strands, and was in all cases conservative for estimating transfer length for 0.5 in. diameter strands. Measured slip values for the slabs manufactured using a slip-form process, on the other hand, showed a much greater variability compared to the measured slips in the extruded slabs. Calculated transfer length for 0.5 in. diameter strands in the slip-formed slabs with Type 1 fibers was close to $50d_b$. Measured slip values for the slabs with Type 2 fibers, on the other hand, were significantly greater than those in the slabs with Type 1 fibers, with calculated transfer lengths exceeding in most cases $80d_b$. This is believed to have been caused by the difficulties encountered in the manufacturing of the slabs with Type 2 fibers, which were twice as long as the Type 1 fibers.

Extruded fiber-reinforced concrete slabs with Type 1 and Type 2 fibers at a 0.38% and 0.30% volume fraction, respectively, exhibited peak shear strengths that ranged between 1.08 and 1.20 times the calculated web-cracking shear strength. The two extruded slabs without fibers, on the other hand, failed at shear forces corresponding to 0.93 and 0.87 times the calculated web-cracking shear strength, V_{cw}. The extruded slabs with Type 2 fibers at 0.38% and 0.50% volume fraction showed a greater variability in shear strength, likely due to variations in fiber distribution or concrete compaction. These slabs failed at shear strengths ranging between 0.94

and $1.29V_{cw}$. Besides an increase in shear strength, the presence of fibers, particularly of Type 2 fibers, led to a more gradual post-peak strength decay.

The test slip-formed slabs that failed in shear exhibited peak shear forces ranging between 0.80 and $1.21V_{cw}$ for an average value of $1.04V_{cw}$. The three spans reinforced with Type 1 fibers that failed in shear (all with fibers at 55 lbs/yd^3 or 320 N/m^3) for which transfer lengths were, on average, approximately $50d_b$, exhibited peak shear forces ranging between 1.08 and $1.21V_{cw}$. A greater variability of shear strength was observed in the slabs with Type 2 fibers, for which significantly larger transfer lengths were calculated.

Even though no regular concrete slip-formed slab was tested as part of this investigation, a comparison of the shear strength of the spans that exhibited a web-cracking shear failure with that of eight slip-formed slabs tested by Palmer and Schultz (2010) suggests that the use of fiber reinforcement leads to an increase in shear strength, especially when considering the slabs with Type 1 fibers for which similar transfer lengths were calculated. The limited data suggest that slabs with Type 1 and Type 2 fibers in the dosages evaluated should lead to shear strengths of at least V_{cw}, as long as transfer lengths of approximately $50d_b$ or shorter can be achieved.

1. INTRODUCTION

Precast, prestressed concrete hollow-core slabs are commonly used in residential, office and industrial construction because of their light weight, rapid construction, and large span-to-depth ratios. Further, the flat top and bottom surfaces of hollow-core slabs require little or no finishing depending on architectural requirements, adding additional benefits in terms of construction time and cost.

The manufacturing of precast, prestressed concrete hollow-core slabs is typically performed using either an extrusion (e.g., Elematic) or a slip-form process. In both cases, nearly zero-slump concrete is used and the manufacturing process allows only the use of longitudinal reinforcement. The presence of hollow cores and the impossibility of placing stirrups in hollow-core slabs makes these members susceptible to shear failures, particularly near the supports, over the transfer length of the prestressing strands where the effective prestressing force has not been fully transferred to the concrete. Moreover, results from past research (Hawkins and Ghosh, 2006) indicated that hollow-core slabs with overall thickness greater than or equal to 12.5 in. (320 mm) may fail at shear forces substantially lower than the web-cracking shear strength, V_{cw}, calculated according to the ACI Building Code. Based on this research, starting with the 2008 ACI Building Code, transverse reinforcement is required in hollow-core slabs with overall depth greater than 12.5 in. where $V_u > 0.5\phi V_{cw}$. Given the fact that the use of bar-type transverse steel is not feasible in most hollow-core slabs, this provision effectively reduces the design web-cracking shear strength by 50% compared to other prestressed concrete members. Similar findings regarding the reduced web-cracking shear strength of deep hollow-core slabs have also been reported in Palmer and Shultz (2011) and Dudnik, Milliman, and Parra-Montesinos (2017).

The most common alternative to date to increase the shear strength of hollow-core slabs is by filling the cores with grout or concrete at the ends of the member. While effective, this solution is time consuming and increases the weight of the member, thereby diminishing one of the major advantages of hollow-core slabs, which is their light weight. Another alternative that has been investigated in the past few years is the use of discrete, randomly oriented steel fibers added to the concrete mixture (e.g., Peaston, Elliott and Paine, 1999; Cuenca and Serna, 2013; Simasathien and Chao, 2015; and Dudnik, Milliman, and Parra-Montesinos, 2017). In general,

the use of hooked steel fibers in volume fractions between 0.5% and 1.0% has led to an increase in shear strength and ductility in hollow-core slabs.

To the writers' knowledge, however, the only laboratory study conducted on fiber-reinforced concrete hollow-core slabs with overall depths greater than 12.5 in. was that by Dudnik, Milliman, and Parra-Montesinos (2017), where six tests on extruded 16-in. deep slabs were conducted. Two shear span-to-depth ratios were evaluated, 3.0 and 3.5. For each shear span-to-depth ratio, three shear spans were tested, one without fibers, one with fibers at 66 lbs/yd^3 (385 N/m^3) or at a 0.5% fiber volume fraction, and one with fibers at 100 lbs/yd^3 (585 N/m^3) or at a 0.76% fiber volume fraction. The steel fibers used had hooks at their ends. The fiber length, diameter and nominal ultimate strength were, respectively, 1.18 in. (30 mm), 0.022 in. (0.55 mm), and 160 ksi (1100 MPa). The slabs were simply supported and subjected to a monotonically increased concentrated force at the end of the shear span.

Figure 1 shows the applied shear, normalized by the calculated web-cracking shear strength according to ACI 318-14, V_{cw}, versus deflection under the load for the tests with shear span-to-depth ratio of 3.5. Similar results were obtained for the tests with a shear span-to-depth ratio of 3.0. As can be seen, the slab without fibers failed at approximately 70% of the calculated web-cracking shear strength, V_{cw}, while the slabs with fibers failed at shear forces greater than V_{cw}. It should be noted that the slab with 66 lbs/yd^3 (385 N/m^3) of steel fibers exhibited a greater shear strength than that with steel fibers at 100 lbs/yd^3 (585 N/m^3). This was due to difficulties in the mixing of steel fibers for the latter case, which led to some voids at various locations over the shear span. The substantial increase in shear strength attained through the addition of steel fibers was attributed to the ability of fibers to transfer tension across web diagonal cracks. In the slabs without fibers, diagonal cracking of a single web led to a "zipper" effect, triggering the immediate cracking of the other webs and subsequent failure of the slab. In the case of the slabs with fibers, once one of the webs cracked, the fibers were able to transfer significant tension across the diagonal crack, which allowed the slab to carry additional load. It was only after all webs cracked that a drop in the applied load occurred.
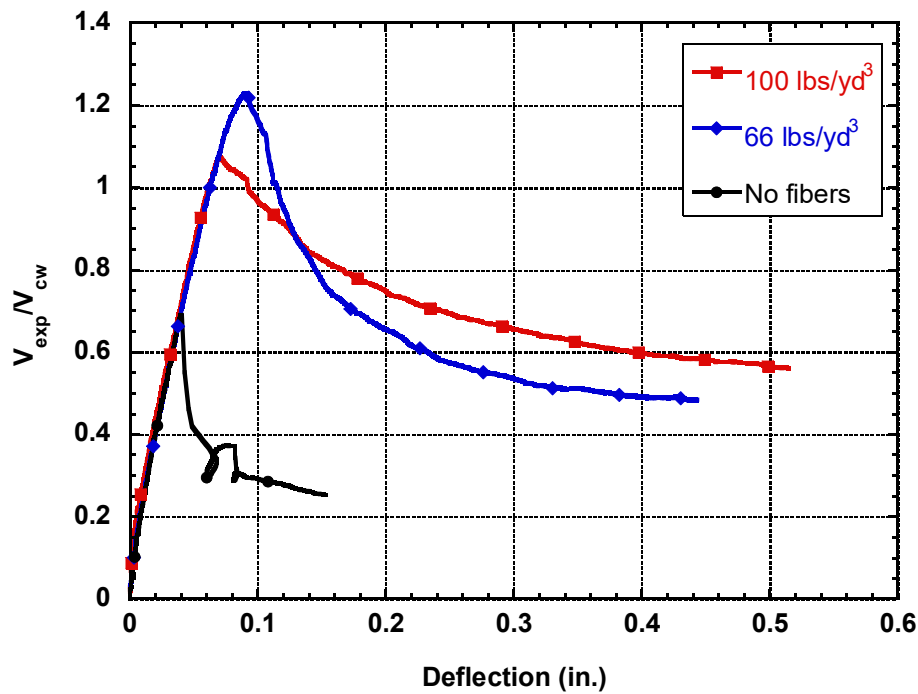
Figure 1 - Normalized shear force versus deflection response for 16-in. deep hollow-core slabs (Dudnik, Milliman, and Parra-Montesinos, 2017)

The tests reported in Dudnik, Milliman, and Parra-Montesinos (2017) gave clear indication that there is potential for the use of deformed steel fibers to increase the shear strength of deep hollow-core slabs. This led to the initiation of a new experimental research study, reported herein, to further evaluate experimentally the shear strength of extruded hollow-core slabs constructed with different steel fibers and at various dosages. Further, as many hollow-core slabs in the USA are manufactured using a slip-form process, the feasibility of using steel fibers as minimum shear reinforcement in slip-formed hollow-core slabs was also evaluated.

3

2. EXPERIMENTAL PROGRAM AND RESULTS

2.1   Experimental Program

The behavior of prestressed, steel fiber reinforced concrete hollow-core slabs was evaluated through two series of tests. Slabs in Series 1 were constructed using an extrusion (Elematic) process, while the slabs in Series 2 were constructed using a slip-form technique. In the slabs manufactured following an extrusion process, augers on the extrusion machine create the hollow cores as the machine moves along the prestressing bed. In the slip-form process used in Series 2, on the other hand, the bottom flange, webs, and top flange are cast separately in that order, while the machine advances along the prestressing bed. In both cases, near zero-slump concrete is required in order to ensure that the concrete stays in place immediately after casting.

For each series, all slabs were manufactured on the same day and along the same prestressing bed. However, the two series were fabricated by two different manufacturers. Because the test slabs had to be cast at the same time as other slabs being manufactured by the precast concrete producer, the design of the slabs in terms of number, diameter, location, and debonded length (if applicable) of the strands was dictated by the design of the slabs being manufactured that day.

The same concrete mixture was used for all the slabs in each series, regardless of the presence of fibers. Because different fiber types and dosages were used, a transition length of approximately 5 ft (1520 mm) was provided between each type of slab in order to ensure that the intended material was the one present at each end.

The main experimental variables evaluated for each series were fiber type and dosage, and shear span-to-effective depth (a/d) ratio.

2.1.1   Series 1 tests

Seven 16-in. (400 mm) deep, prestressed extruded hollow-core slabs were tested to failure in Series 1. Figure 2 shows the cross-section for these slabs. The slabs were reinforced with eleven 7-wire, 270-ksi (1860-MPa) low-relaxation strands. The two exterior strands were 0.5 in. (13 mm) in diameter, while the nine interior strands were 0.6 in. (150 mm) in diameter for a total

area of 2.25 in^2 (1452 mm^2). Prior to casting of concrete, these strands were tensioned to a stress of 0.65f_{pu} or 175.5 ksi (1210 MPa), where f_{pu} is the ultimate strength of the prestressing steel.
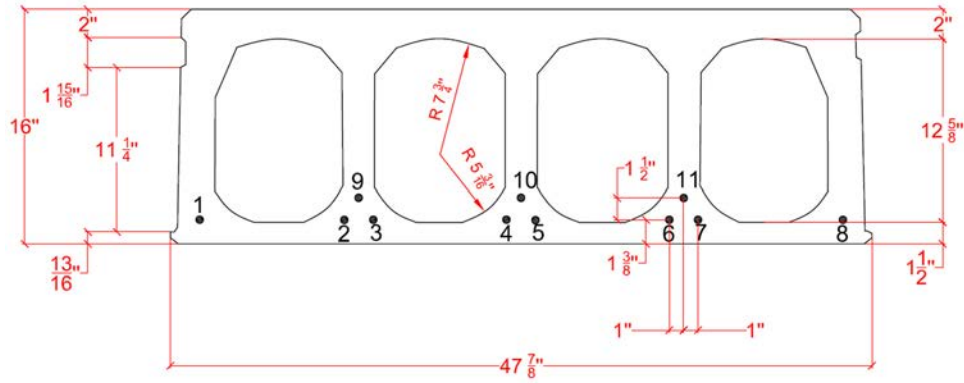
Strands 1 and 8 had a diameter of 0.5 in. (13 mm), while all other strands had a diameter of 0.6 in. (15 mm)

Figure 2 – Cross section for hollow-core slabs in Series 1

Each slab was tested at both ends, for a total of 14 tests. A summary of the main features of each test is presented in Table 1. The specimen designation rules used are as follows. The first letter-number group refers to the test series (S1 for Series 1). The second letter-number group refers to the fiber type (F1 for fiber type 1 and F2 for fiber type 2). The subsequent number refers to the fiber dosage in lbs/yd^3, followed by the shear span-to-effective depth ratio. If a letter is added at the end, it means that more than one nominally identical shear span was tested, with *a* referring to one test shear span and *b* to the nominally identical shear span tested. Thus, test span S1-F2-40-3.0a refers to one of two spans (letter *a* at the end) in Series 1 with Type 2 fibers at 40 lbs/yd^3 and a shear span-to-effective depth ratio of 3.0.

Twelve tests were performed on shear spans cast with steel fiber reinforced concrete, while two tests were conducted on shear spans without fibers. Two types of steel fibers were evaluated in Series 1 tests. Type 1 fibers were 1.18 in. (30 mm) long, 0.022 in. (0.55 mm) diameter steel fibers with hooked ends (Fig. 3). The wire used to manufacture these fibers had a nominal tensile strength of 160 ksi (1100 MPa). Type 2 fibers, on the other hand, were 2.36 in. (60 mm) long and 0.035 in. (0.9 mm) in diameter, with double hooks at each end. The nominal tensile strength for Type 2 fibers was 335 ksi (2300 MPa). It is worth mentioning that Type 1 fibers are expected to

slip while remaining elastic (except for the hooked ends) as cracks in the concrete widen. On the other hand, because the double hooks in the Type 2 fibers are expected to prevent these fibers from slipping, significant crack opening would lead to yielding and potential fracture of these fibers.

Table 1 – Summary of Series 1 tests

Span ID	a (in.)	a/d	L_{end} (in.)	L_1 (in.)	L_2 (in.)	f'_c (psi)	V_{exp} (kips)	V_{cw} (kips)	V_{exp}/V_{cw}
S1-NF-3.0	42.0	3.0	1.75	96.0	82.3	13,100	75.0	80.9	0.93
S1-NF-3.5	49.0	3.5	1.75	103.0	75.3		70.1	80.5	0.87
S1-F1-50-3.0	42.0	3.5	1.75	96.0	82.3	11,390	86.6	76.5	1.13
S1-F1-50-3.5	49.0	3.5	1.75	103.0	75.3		95.1	76.2	1.25
S1-F2-40-3.0a	42.0	3.0	1.75	96.0	82.3	12,290	93.6	78.9	1.19
S1-F2-40-3.5a*	49.0	3.5	38.0	103.0	39.0		121	106	1.13
S1-F2-40-3.0b	42.0	3.0	1.75	96.0	82.3		85.0	78.9	1.08
S1-F2-40-3.5b	49.0	3.5	1.75	103.0	75.3		94.5	78.5	1.20
S1-F2-50-3.0a	42.0	3.0	1.75	96.0	82.3	10,750	71.7	74.8	0.96
S1-F2-50-3.5a	49.0	3.5	1.75	103.0	75.3		69.7	74.5	0.94
S1-F2-50-3.0b	42.0	3.0	1.75	96.0	82.3		96.5	74.8	1.29
S1-F2-50-3.5b	49.0	3.5	1.75	103.0	75.3		84.1	74.5	1.13
S1-F2-62-3.0	42.0	3.0	1.75	96.0	82.3	12,570	87.1	79.6	1.09
S1-F2-62-3.5	49.0	3.5	1.75	103.0	75.3		100	79.2	1.26

*Cores were filled at the slab end.
See Fig. 4 for L_{end}, L_1 and L_2.
a: shear span length; d: effective depth; f'_c: cylinder compressive strength; V_{exp}: peak shear force; V_{cw}: calculated web-cracking shear strength according to ACI 318-14.

As shown in Table 1, Type 1 fibers were evaluated at 50 lbs/yd³ or 290 N/m³ (0.38% volume fraction), while Type 2 fibers were evaluated at 40, 50 and 62 lbs/yd³ (230, 290 and 360 N/m³) for fiber volume fractions of 0.30, 0.38 and 0.50%, respectively. Both fiber types were delivered in bundles, with fibers glued to each other by a water-soluble glue that dissolved when in contact with water to improve fiber distribution.
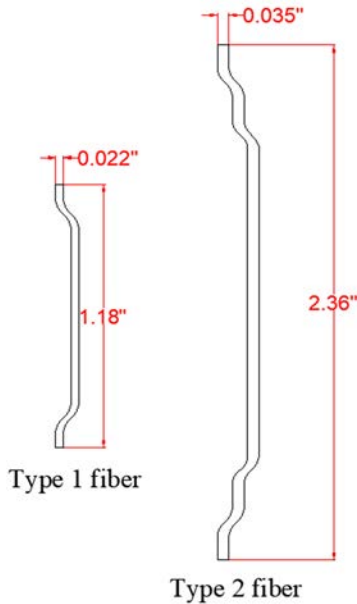
Figure 3 - Type 1 and Type 2 fibers

The same concrete mixture was used for all Series 1 slabs, regardless of the presence of fibers. In general, no major issues were encountered with the manufacturing of the slabs, which is consistent with previous observations (Dudnik, Milliman, and Parra-Montesinos, 2017) for slabs with Type 1 fibers in dosages of up to 66 lbs/yd^3 (385 N/m^3).

The setup used in the slabs in Series 1 is shown in Fig. 4. Each slab had a total length of 15 ft (4570 mm). The first test was conducted on a shear span with a length of 3.0d, with a distance between supports of 96 in. (2440 mm). As show in Fig. 4, the other end of the slab was cantilevered in order to prevent any damage to this end during the first test. Once the first test was completed, the supports were relocated and the slab moved for testing of the other end, with a shear span of 3.5d. The bearing surface at the test end consisted of a 1.5 in. (38 mm) wide and 0.2 in. (5 mm) thick multi-monomer plastic bearing pad seating on top of a 6 in. (150 mm) wide, 1 in. (25 mm) thick steel plate. This steel plate was in turn placed on top of a 3/4 in. (19 mm) diameter steel roller. Except for one slab end that had the cores filled, the distance between the center of the support and the edge of the slab was 1.75 in. (45 mm). For the slab end with filled cores, this distance was 38.0 in. (965 mm) in order to test the region with hollow cores.

7
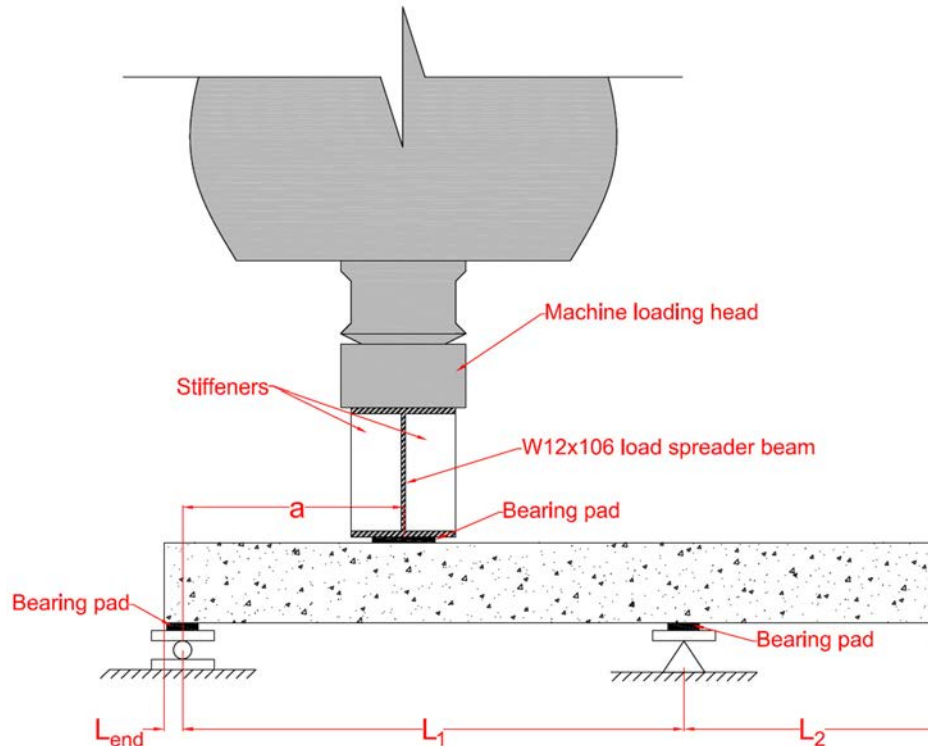
Figure 4 – Sketch of test setup for Series 1 tests

Load was applied through a 1000-kip (4450-kN) testing machine at a constant displacement rate of 0.03 in./min (0.76 mm/min). As shown in Fig. 5, a steel spreader beam was placed underneath the 12 in. (305 mm) diameter crosshead of the hydraulic actuator in order to spread the load across the entire width of the slab. A 6 in. (150 mm) wide, 0.5 in. (13 mm) thick commercial grade 200 neoprene bearing pad was placed between the spreader beam and the slab in order to achieve a more uniform distribution of the load. This test setup was very similar to that used in a previous investigation on the shear behavior of fiber reinforced concrete hollow-core slabs (Dudnik, Milliman, and Parra-Montesinos, 2017), which allows for comparison of test results.

2.1.2 Series 2 tests

Eight slabs were manufactured using a slip-form process for a total of 16 tests in Series 2. The cross section for these slabs is shown in Fig. 6. Although each slab was reinforced with twelve 0.5 in. diameter strands, four of these strands (3, 4, 9, and 10) were debonded using a concrete retarder throughout their entire lengths. Further, strands 5 and 8 were also debonded over 2 ft

(610 mm) from each end, except for Slab S2-F2-40-2.8, for which these two strands were fully bonded along their length. The strands were subjected to an initial prestress of 186 ksi (1280 MPa). It should be emphasized that the strand layout and debonding scheme used was governed by the design of additional slabs that were manufactured in the same prestressing bed.
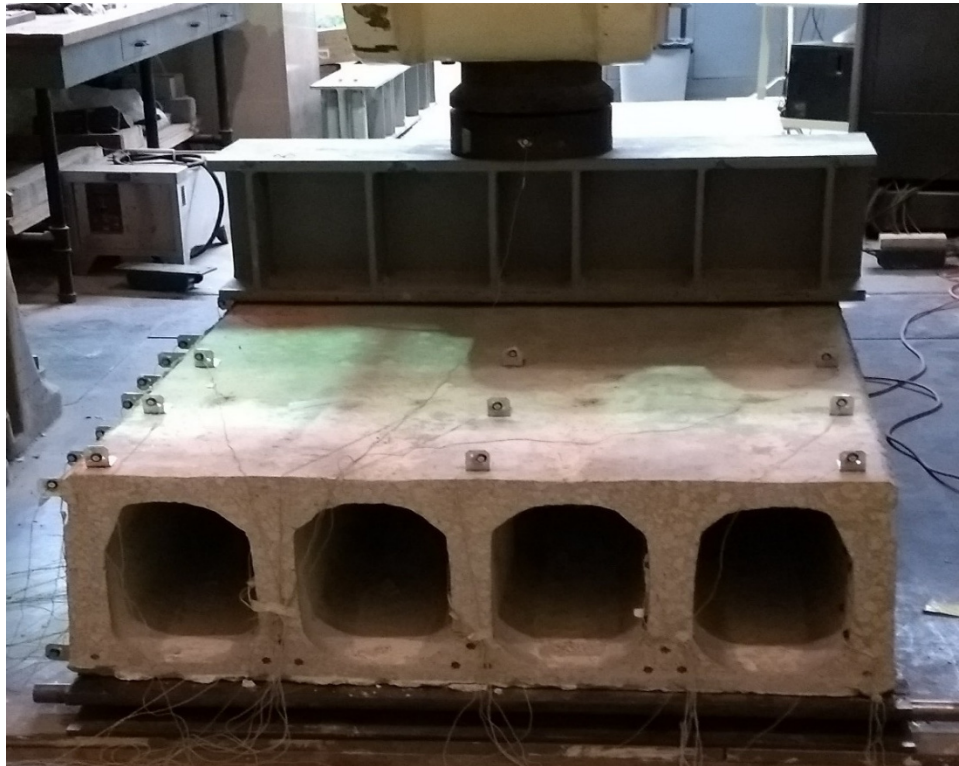
Figure 5 – Hollow-core slab in Series 1 prior to testing
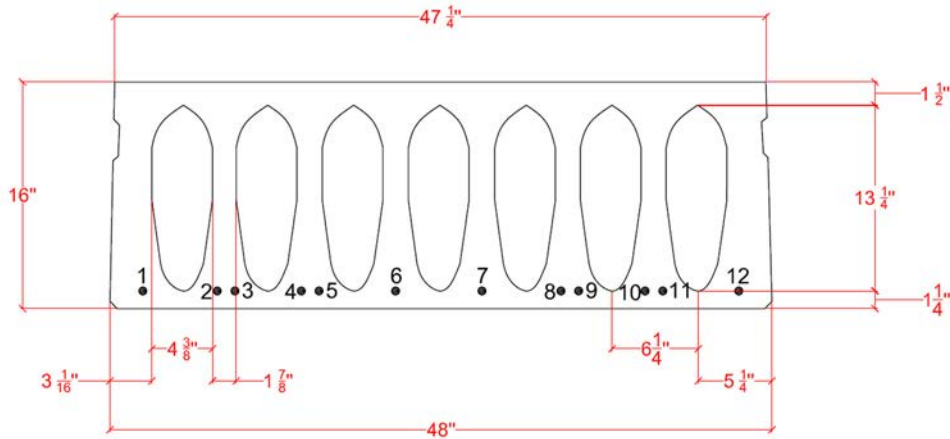
All strands 0.5 in. (13 mm) in diameter.
Strands 3, 4, 9, and 10 were fully unbonded along the span length
Strands 5 and 8 were debonded over 2 ft (610 mm) from the slab edge, except for test span
S2-F2-40-2.8a

Figure 6 – Cross section for hollow-core slabs in Series 2

The same two types of fibers used in Series 1, Type 1 and Type 2 fibers, were also evaluated in Series 2. Type 1 fibers were evaluated at 55 and 66 lbs/yd³ (320 and 385 N/m³), which corresponded to a fiber volume fraction of 0.42 and 0.50%, respectively. Type 2 fibers, on the other hand, were evaluated at 40 and 50 lbs/yd³ (230 and 290 N/m³), which corresponded to a fiber volume fraction of 0.30 and 0.38%, respectively. No major issues were faced in the manufacturing of the slabs with Type 1 fibers at 55 lbs/yd³ (320 N/m³). When manufacturing slabs with either larger contents of Type 1 fibers or with Type 2 fibers at both dosages evaluated, however, the machine had to be stopped numerous times due to fibers getting stuck in the machine. This was particularly important for the slabs with Type 2 fibers, which affected the cross-section of the slabs (Fig. 7) and could have influenced the performance observed in tests.

Figure 7 – Flange defects in a slab manufactured using a slip-form process

A summary of the main features of each test in Series 2 is provided in Table 2. The same specimen designation rules used in Series 1 were used in Series 2. As can be seen, *a/d* ratios for the tests in this series ranged between 2.0 and 3.0. As will be discussed later, the first three spans tested as part of this series failed in flexure. In order to increase the flexural strength of the slabs, three shear spans were tested with the support moved in to increase the available bonded length of the strands up to the load point. Further, in the remaining ten tests, an external prestressing force of 80 kips (360 kN) was applied through several prestressing rods placed at approximately 3 in. (76 mm) from the bottom of the slab (Fig. 8).

Table 2 – Summary of Series 2 tests

Span ID	a (in.)	a/d	L_{end} (in.)	L_1 (in.)	L_2 (in.)	f'_c (psi)	V_{exp} (kips)	V_{cw} (kips)	V_{exp}/V_{cw}
S2-F1-55-2.0a†	28.0	2.0	48.0	80.0	52.0		116	107.7	1.08
S2-F1-55-2.0b†	28.0	2.0	48.0	80.0	52.0	8750	121	107.7	1.13
S2-F1-55-2.8*	39.2	2.8	1.75	91.2	87.1		116	103.0	1.12
S2-F1-55-3.0**	42.0	3.0	1.75	94.0	84.3		125	103.2	1.21
S2-F1-66-2.3†	32.2	2.3	1.75	84.2	94.1		67.8	92.9	0.72
S2-F1-66-2.8a†	39.2	2.8	1.75	91.2	87.1		71.0	103.0	0.77
S2-F1-66-2.8b†	39.2	2.8	43.5	91.2	45.3	9450	110	110.7	0.99
S2-F1-66-2.8c*	39.2	2.8	1.75	91.2	87.1		122	106.2	1.15
S2-F1-66-3.0*	42.0	3.0	1.75	94.0	84.3		102	106.1	0.96
S2-F2-40-2.8a†	39.2	2.8	1.75	91.2	27.1		77.6	108.3	0.72
S2-F2-40-2.8b**	39.2	2.8	1.75	109.2	69.1	9600	125	107.0	1.16
S2-F2-40-3.0*	42.0	3.0	1.75	112.0	66.3		95.7	106.8	0.89
S2-F2-50-2.8a*	39.2	2.8	1.75	91.2	87.1		106	112.1	0.95
S2-F2-50-2.9*	40.6	2.9	1.75	92.6	85.7	10,800	89.0	112.9	0.80
S2-F2-50-2.8b*	39.2	2.8	1.75	93.2	87.1		103	112.1	0.92
S2-F2-50-3.0*	42.0	3.8	1.75	42.0	84.3		122	111.9	1.09

*In addition to the pretensioned force, an 80-kip postensioned force was applied through 4 Dywidag rods (Fig. 8).
** In addition to the pretensioned force, an 80-kip postensioned force was applied through 3 Dywidag rods.
See Fig. 4 for L_{end}, L_1 and L_2.
a: shear span length; d: effective depth; f'_c: cylinder compressive strength; V_{exp}: peak shear force; V_{cw}: calculated web-cracking shear strength according to ACI 318-14.
†Bearing pad at test support consisted of a 2.0 in. (50 mm) wide neoprene pad. For all other tests, a 1.5 in. (38 mm) wide multi-monomer plastic bearing pad was used.

Figure 8 - External prestressing applied to hollow-core slabs in Series 2

The setup used in the Series 2 tests was very similar to that used in Series 1. However, in some of the slabs, the bearing pad in the support of the test shear span consisted of a 2.0 in. (50 mm) wide, 0.5 in. thick neoprene bearing pad (see Table 2).

2.1.3   Instrumentation

Applied loads were measured through a load cell connected to the 1000 kip (4450 kN) testing machine. Slab deflections and deformations, on the other hand, were calculated using measurements from a non-contact position tracking system (Northern Digital Inc., 2011). This system tracked the position in space of markers attached to the top and one side surface of the slab. Reported deflection values correspond to deflections at or very near the loading point relative to the support at the end of the test shear span. Markers were also attached to the inner webs of the Series 1 slabs in an attempt to track the formation of diagonal cracks close to the support. Markers could not be used in the inner webs of the Series 2 slabs because of the narrow hollow cores in the Series 2 slabs, which prevented the markers from being detected by the system cameras.

2.2   Material Properties

Compressive strength for the concrete used in the slabs of Series 1 and 2 were obtained through testing of 6 in. x 12 in. cylinders. The compressive strengths obtained at or near the day of testing of the shear spans in Series 1 and 2 are listed in Tables 1 and 2, respectively. Concrete compressive strength ranged between 10,750 and 13,100 psi (74.1 and 90.3 MPa) for the slabs in Series 1, and between 8750 and 10,800 psi (60.3 and 74.4 MPa) for the slabs in Series 2. All strands used in the slabs of Series 1 and 2 were 270-ksi (1860-MPa) low-relaxation strands.

The tensile performance of the various fiber reinforced concretes used was evaluated indirectly through three- or four-point bending tests of 6 in. x 6 in. x 20 in. (150 mm x 150 mm x 510 mm) beams. The results from these tests, however, should be taken with caution given the nearly zero slump of the concretes used, which made casting of these beams very difficult even with the application of external vibration. Further, the process of manufacturing these beams cannot be

13

consider representative of the process used to cast the concrete in the hollow-core slabs, in which either an extrusion or slip-form process was used.

Average equivalent bending stress versus deflection responses for the fiber reinforced concretes used in Series 1 slabs are shown in Fig. 9a. Equivalent bending stress was calculated assuming linear elastic behavior and using uncracked section properties. The responses of individual beams from which the average was obtained were relatively consistent for each material, with deviations from the average less than ±75 psi (0.52 MPa) in the post-cracking range, except for one of the three beams with Type 2 fibers at 66 lbs/yd^3 (385 N/m^3), which showed a maximum deviation of nearly +200 psi (1.4 MPa) from the average at a mid-span deflection of approximately 0.06 in. (1.5 mm). It should be noted that the beams with Type 2 fibers at 66 lbs/yd^3 (385 N/m^3) were tested under four-point bending, as specified in ASTM C1609/C1609M-12, while the rest of the beams were erroneously tested under three-point bending. As can be seen in Fig. 9a, the behavior of the fiber reinforced concretes with Type 2 fibers was significantly better than that of the concrete with Type 1 fibers, even when Type 2 fibers were used at a 20% lower dosage. Increases in the dosage of Type 2 fibers, however, did not translate into a substantial improvement in performance. It possible that this was caused by difficulties in mixing the fiber reinforced concretes with higher dosages of Type 2 fibers.

Average equivalent flexural stress versus midspan deflection responses from four-point bending tests for the fiber reinforced concretes in Series 2 with Type 1 fibers at 55 and 66 lbs/yd^3 (320 and 385 N/m^3), and Type 2 fibers at 40 lbs/yd^3 (230 N/m^3) are shown in Fig. 9b. No data were available for the material with Type 2 fibers at 50 lbs/yd^3 (290 N/m^3) because no beam samples could be taken for this material. Two beams were tested for each concrete type.
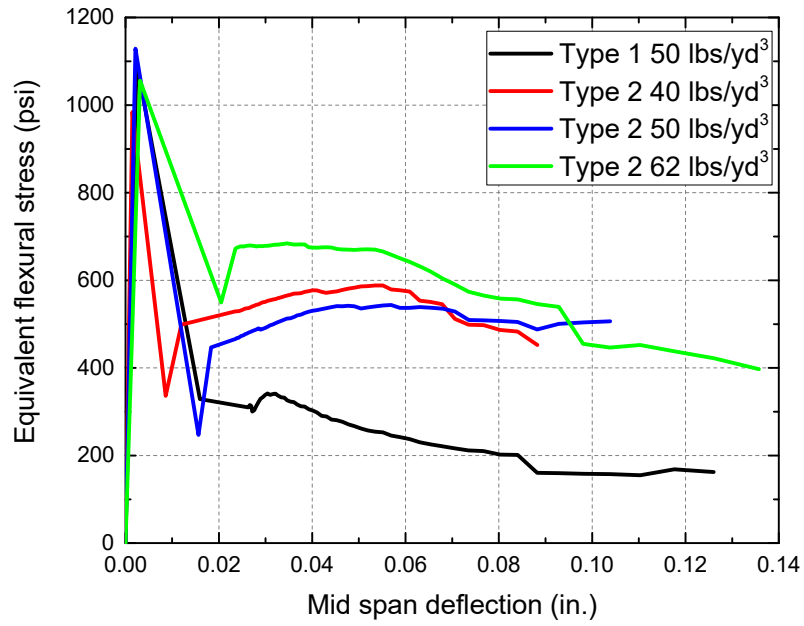
a)   Series 1
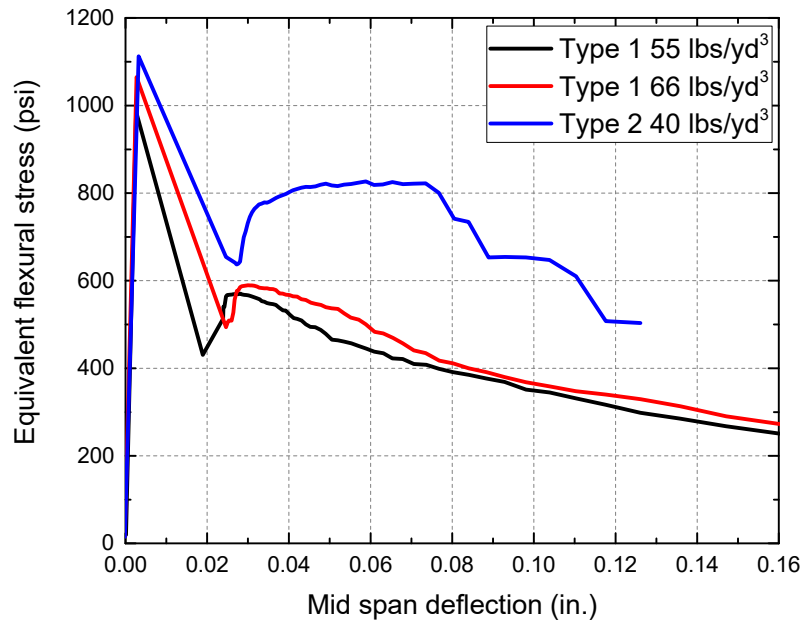
b)   Series 2

Figure 9 - Average equivalent flexural stress versus deflection response for materials used in Series 1 and 2

15

The behavior of the Series 2 beams with Type 1 fibers was very consistent in the post-cracking range, with a maximum deviation from the average of approximately ±50 psi (0.35 MPa). The behavior of these beams was characterized by a sharp drop in stress right after first cracking, followed by a gradual stress decrease as midspan deflection was increased. The average equivalent flexural stress versus midspan deflection response of the two concretes with Type 1 fibers was very similar, even though there was a 20% difference in fiber content. For the concrete with Type 2 fibers, on the other hand, maximum deviation from the average was ±125 psi (0.86 MPa). As expected, the use of Type 2 fibers led to significantly better post-cracking behavior, even though these fibers were used at a lower dosage compared to those for Type 1 fibers. The beams with these fibers exhibited a significant regain in strength after a pronounced stress drop at first cracking, followed by a gradual stress decrease for deflections larger than approximately 0.075 in. (1.9 mm). However, the average post-cracking peak stress for these beams was only approximately 75% of the first cracking strength.

Compared with the beams tested for Series 1 with Type 1 fibers at 62 lbs/yd^3 (385 N/m^3) and Type 2 fibers at 50 lbs/yd^3 (290 N/m^3), the behavior of the beams in Series 2 was significantly better. It is possible that this difference was caused by the fact that the concrete mixture used in the slip-form process was slightly more workable than that used in the extrusion process, leading to a better compaction of the beam samples.

2.3   Strand End Slips

End slip for the strands in the test slabs was measured in order to estimate transfer length and evaluate whether the presence of fibers led to a change in bond conditions at the end of the slabs. Although the presence of fibers has been reported to enhance bond between concrete and prestressing strands (Chao, Naaman and Parra-Montesinos, 2006), this may not be the case in hollow-core slabs given the near-zero slump of the concrete and the increase in stiffness of the mixture due to the addition of fibers, which may affect concrete compaction. Dudnik, Milliman and Parra-Montesinos (2017) reported that end slip was not significantly affected by the presence of fibers (Type 1 in this study) when used in volume fractions of up to 0.50%. However, a significant increase end slip was observed in slabs with Type 1 fibers at a 0.76% volume fraction

due to compaction problems associated with the poor workability of the steel fiber reinforced concrete.

Figures 10a and 10b show the average measured end slips for slabs in Series 1 and 2. The slip values reported are lumped into average slips for each concrete material used, which were calculated as the average of the slips measured at both ends of the same strand for all slabs cast using the same material. It should be mentioned, however, that for Series 2, strand slip data were not available for the slabs with Type 2 fibers at a 0.30% volume fraction. Also shown in the figures are the calculated slips corresponding to an effective prestress of 95% of the initial prestress (167 ksi or 1150 MPa for Series 1 slabs and 178 ksi or 1230 MPa for Series 2 slabs) and a transfer length of $50d_b$, where d_b is the strand diameter.

As can be seen in Fig. 10a, slip values in the slabs constructed using an extrusion process did not seem to be affected by the presence of fibers. It should be noted that all strands in these slabs had a diameter of 0.6 in., except for strands 1 and 8, which were 0.5 in. in diameter. In general, $50d_b$ represented an adequate, and often conservative estimation of the average transfer length for the 0.6 in. diameter strands, and was in all cases conservative for estimating transfer length for the 0.5 in. diameter strands. This is consistent with previous slip data reported by Dudnik, Milliman and Parra-Montesinos (2017) on extruded regular concrete and fiber-reinforced concrete hollow-core slabs.

Measured slip values for the slabs manufactured using a slip-form process showed a much greater variability compared to the measured slips in the extruded slabs (Fig. 10b). Measured slips in the bonded and partially debonded strands were smallest for the strands in the slabs with Type 1 fibers at 55 lbs/yd^3 (320 N/m^3), with values near or below that corresponding to a transfer length of $50d_b$, except for the strands at the edges of the slab. The strands in the slabs with Type 1 fibers at 66 lbs/yd^3 (385 N/m^3) showed a similar trend, but with larger slip values that in most cases exceeded that corresponding to a transfer length of $50d_b$. Measured slip values for the slabs with Type 2 fibers at 50 lbs/yd^3 (290 N/m^3), on the other hand, were significantly greater than those in the slabs with Type 1 fibers. This is believed to have been caused by the difficulties encountered in the manufacturing of the slabs with these fibers, which were twice as long as the Type 1 fibers. The calculated transfer length for most of the strands in these slabs exceeded $80d_b$. Slip values for the fully unbonded strands (3, 4, 8, and 9), as expected were significantly larger,

indicating negligible transfer of prestressing force at the end of the slabs. It seems, however, that these strands had a minor contribution to effective prestress in the region close to the loading point.
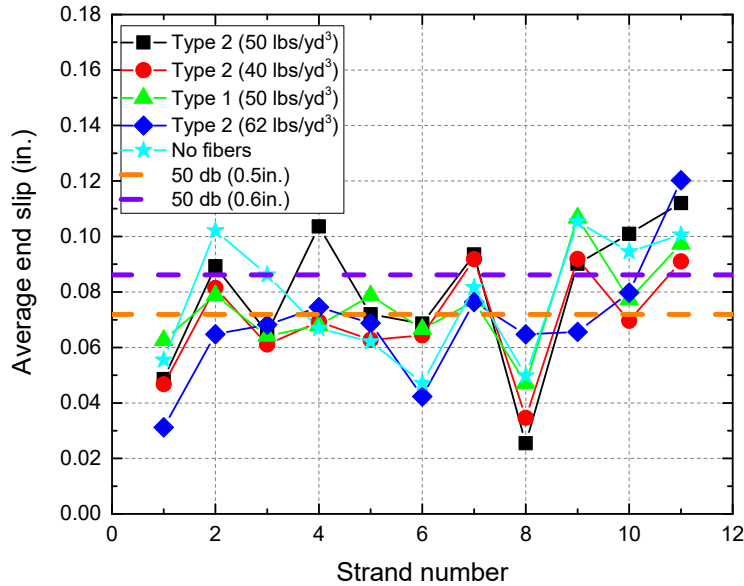
All strands were 0.6 in. (15 mm) in diameter, except for strands 1 and 8, which were 0.5 in. (13 mm) in diameter.
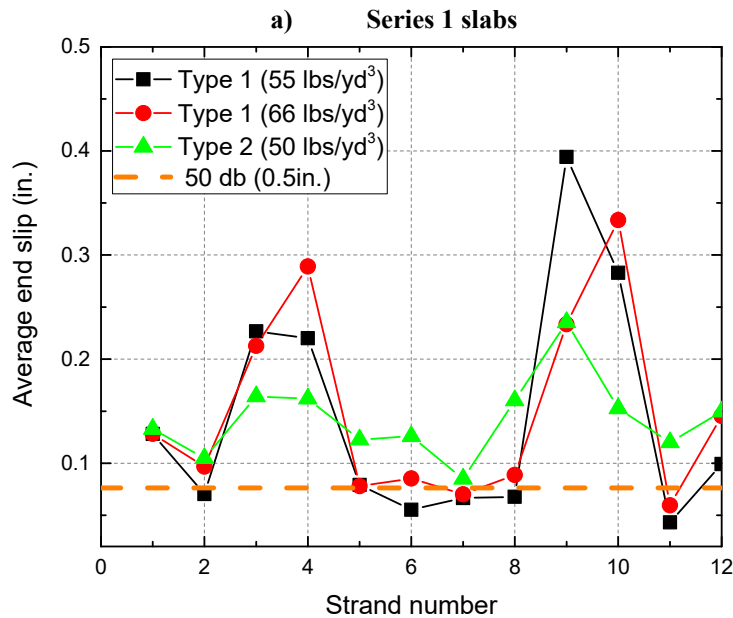
a)   Series 1 slabs

Strands 3, 4, 9, and 10 were fully unbonded along the span length
Strands 5 and 8 were debonded over 2 ft (610 mm) from the slab edge, except for test span S2-F2-40-2.8a

b)   Series 2 slabs

Figure 10 - Average strand end slip for Series 1 slabs

18

Because no regular concrete slabs were manufactured using a slip-form process, the effect fibers may have had on transfer length could not be evaluated. It should be mentioned, however, that Palmer and Schultz (2010) reported slip values for 16 in.-deep (405 mm) regular slip-formed concrete slabs (no fibers) that corresponded, on average, to a transfer length $48d_b$. This is consistent with the transfer lengths calculated for the slabs with Type 1 fibers, particularly at 55 lbs/yd^3 (320 N/m^3), for which no major issues were encountered during manufacturing. It is thus likely that the significantly larger calculated transfer lengths for the slabs with Type 2 fibers was due to compaction problems associated with the use of these longer fibers.

2.4   Calculated Web-Cracking Shear Strength

The experimental shear strengths exhibited by the test slabs was compared with the web-shear shear cracking strength, V_{cw}, calculated according to Section 22.5.8.3.2 of ACI 318-14 as follows,

$$V_{cw} = \left(3.5\lambda\sqrt{f_c'} + 0.3\sigma_g\right)b_w d_p + V_p \tag{1}$$

where λ takes into account the effect of lightweight aggregate ($\lambda = 1.0$ in this case), σ_g is the compressive stress in the concrete at the centroid of the section due to the effective prestressing force, b_w is the web width, d_p is the effective depth, and V_p is the vertical component of the effective prestressing force at the section considered (zero for the test slabs). For the calculation of σ_g, the transfer of effective prestress from the strands to the concrete was assumed to occur over 50 strand diameters from either the end of the strand or the beginning of the bonded portion of the strand for the partially debonded strands used in the Series 2 slabs. For the Series 2 slabs subjected to an external prestressing force of 80 kips (360 kN), this axial force was added to the prestressing force contributed by the strands. Concrete compressive strength used in the calculations corresponded to the measured average cylinder strength. Tables 1 and 2 list the calculated web-cracking shear strengths for the Series 1 and Series 2 tests, respectively.

2.5   Overall Behavior

2.5.1   Series 1 tests

Figures 11a and 11b show the normalized shear force versus deflection responses for the tests with a/d ratio of 3.0 and 3.5 in Series 1, respectively. Individual responses can be found in Appendix A. In these figures, normalized shear force was calculated as the ratio between the applied shear, V_{exp}, and the calculated web-cracking shear strength, V_{cw}. The two test shear spans without fibers, S1-NF-3.0 and S1-NF-3.5, exhibited peak strengths corresponding to 93% and 87% of V_{cw}. It is worth mentioning that two shear spans manufactured at the same facility and tested as part of a previous investigation (Dudnik, Milliman, and Parra-Montesinos, 2017) failed at approximately 70% of V_{cw}. Unfortunately, no explanation could be found for this significant difference in normalized shear strength. The peak shear force in the slabs without fibers corresponded to the load at which web-shear cracking developed near the support (see Fig. 12 for a typical web-shear crack and Appendix B for photos of all cracked shear spans). As also reported in Dudnik, Milliman and Parra-Montesinos (2017), web diagonal cracking occurred on all webs almost simultaneously, as the loss of shear force carried by a web once it cracked led to an overloading of the other webs, creating a "zipper" effect. Application of additional deflection beyond this point led to a rapid decrease in shear force, as shown in Figures 11a and 11b.
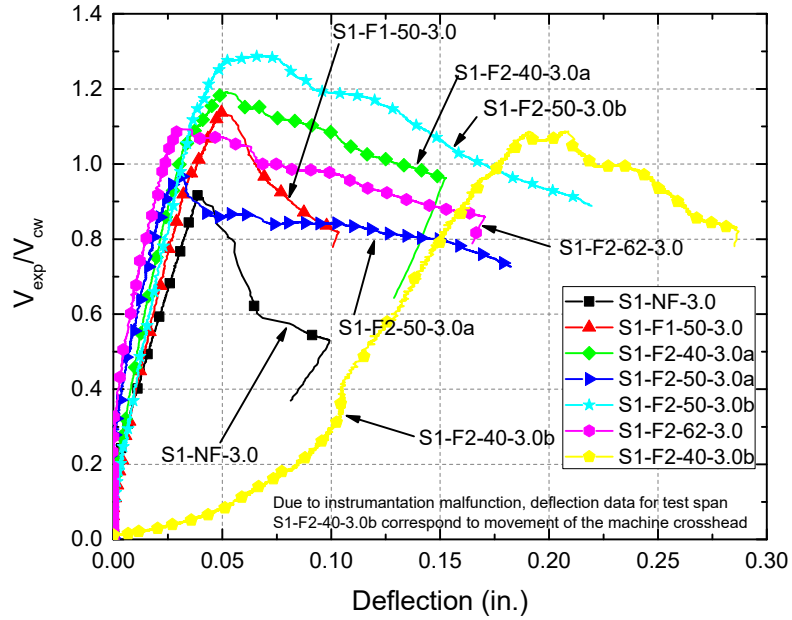
a) a/d=3.0
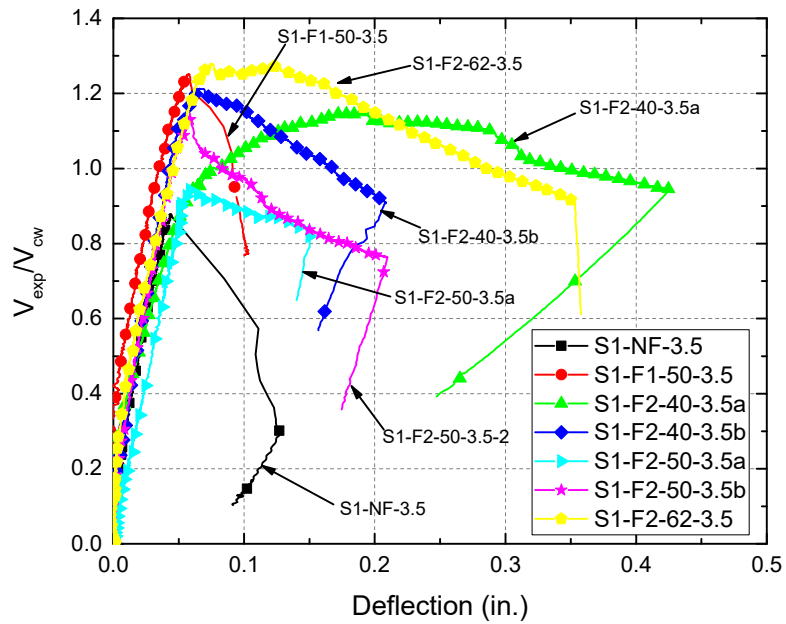
b) a/d=3.5

Figure 11 - Normalized shear force versus deflection response for test spans in Series 1

21

All fiber reinforced concrete test spans in Series 1, with the exemption of spans S1-F2-50-3.0a and S1-F2-50-3.5a, exhibited peak shear strengths that ranged between 1.08 and 1.29 times the calculated web-cracking shear strength. The peak shear strength exhibited by spans S1-F2-50-3.0a and S1-F2-50-3.5a, on the other hand, was 0.96 and 0.94 times the calculated web-cracking shear strength. It should be noted that the normalized shear strength of two nominally identical shear spans, S1-F2-50-3.0b and S1-F2-50-3.5b, was significantly greater (1.29 and $1.13V_{cw}$, respectively). It is possible that the lower shear strengths were due to poor fiber distribution or concrete compaction, especially given the fact that both test shear spans corresponded to the same slab. However, no definite cause could be identified.

Besides an increase in shear strength, the presence of fibers, in particular Type 2 fibers, led to a more gradual post-peak strength decay, as shown in Figs. 11a and 11b. This could be explained by the significantly better post-cracking behavior exhibited by the material test beams with Type 2 fibers (Fig. 9a), as these longer fibers were capable of transferring higher tensile stresses at larger crack widths than the shorter Type 1 fibers. There does not seem to be any correlation, however, between the behavior of the test beams and the web-cracking shear strength of the test shear spans.

Contrary to the slabs without fibers, the presence of fibers, in general, allowed web diagonal cracking to occur progressively rather than nearly simultaneously. Basically, diagonal cracking on a single web did not translate into a sudden loss of web shear strength large enough to immediately overload and cause diagonal cracking of the other webs. It was only after several webs had cracked that the applied load started to decrease. Similar observations were made by Dudnik, Milliman and Parra-Montesinos (2017).

Figure 12- Typical web cracking for test spans in Series 1

2.5.2 *Series 2 tests*

The behavior of the slabs in Series 2 was highly variable and depended primarily on 1) whether or not external prestressing was applied, 2) distance from the support to the slab end, and 3) strand slip. As discussed earlier, external prestressing or an increase in the distance between the support and the edge of the slab were two attempts aimed at increasing the flexural strength of the specimens in order to induce a shear failure, given that the first few spans tested with a 1.75 in. (45 mm) distance between the edge of the slab and the support, without external prestressing, did not exhibit a shear failure. The significant differences in strand anchorage conditions between the slabs with Type 1 and Type 2 fibers, as indicated by the measured strand slips (see Fig. 10b), also influenced the response of the specimens because it affected the buildup of prestressing force in the slab and the flexural strength of the test spans.

Test shear spans without external prestressing

Three of the test shear spans, S2-F1-66-2.8a, S2-F1-66-2.3, and S2-F2-40-2.8a had no external prestressing and a distance between the center of the support and the slab end of 1.75 in. (45

mm). In all three cases, the test spans exhibited a single flexural crack at the location of the applied load (see Appendix B for photos of the cracked shear spans). Following the formation of this crack, the behavior of the slab was governed by strand slip, which led to the opening of that crack and a nearly constant load with increased deflection (Fig. 13). For these test shear spans, the bonded length for the strands up to the loading point was either 82 or 68 strand diameters for the fully bonded strands, and 34 or 20 strand diameters for the partially debonded strands (see Fig. 6 for location of fully bonded versus partially debonded strands). As shown in Table 2, peak loads for these slabs were significantly smaller than the calculated web-cracking shear strength.
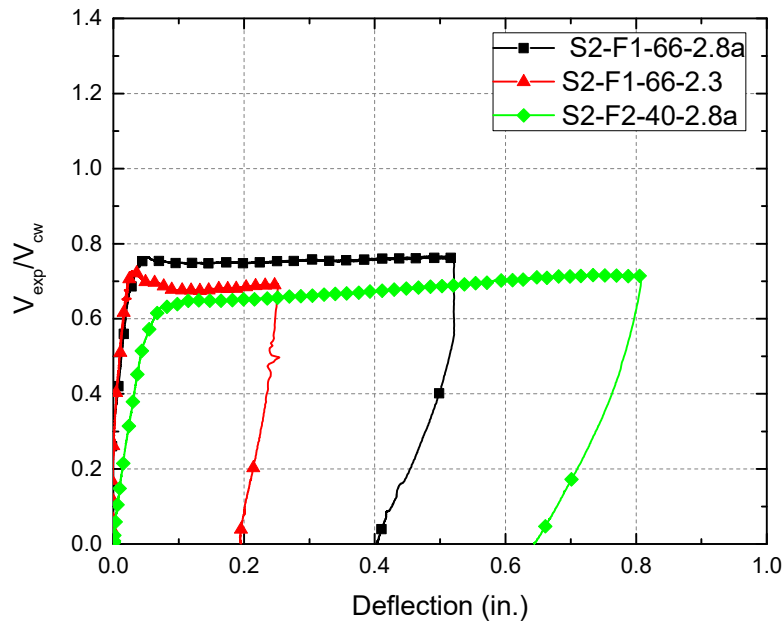
Figure 13 - Normalized shear force versus deflection response for Series 2 test spans without external prestressing and L_{end} = 1.75 in. (45 mm)

Three additional tests in Series 2 were conducted on shear spans without external prestressing, but with a distance between the center of the support and the slab end of either 48 in. (S2-F1-55-2.0a &b) or 43.5 in. (S2-F1-66-2.8b) (1220 or 1105 mm). Because of the increased strand bonded length for these shear spans, flexural cracking strength at the load point was greater than for the three slabs discussed above. Two of these slabs (S2-F1-55-2.0b and S2-F1-66-2.8b), however, exhibited a behavior dominated by strand slip after flexural cracking with a nearly

constant load with increased deflection (Fig. 14). Even though the behavior exhibited by these slabs was controlled by strand slip, the peak shear force was either approximately equal to or greater than the calculated web-cracking shear strength. The other slab in this group, S2-F1-55-2.0a, failed by web-shear cracking at a peak shear force of 1.11 times the calculated web-cracking shear strength, which led to a pronounced decreased in the applied load (Fig. 14).
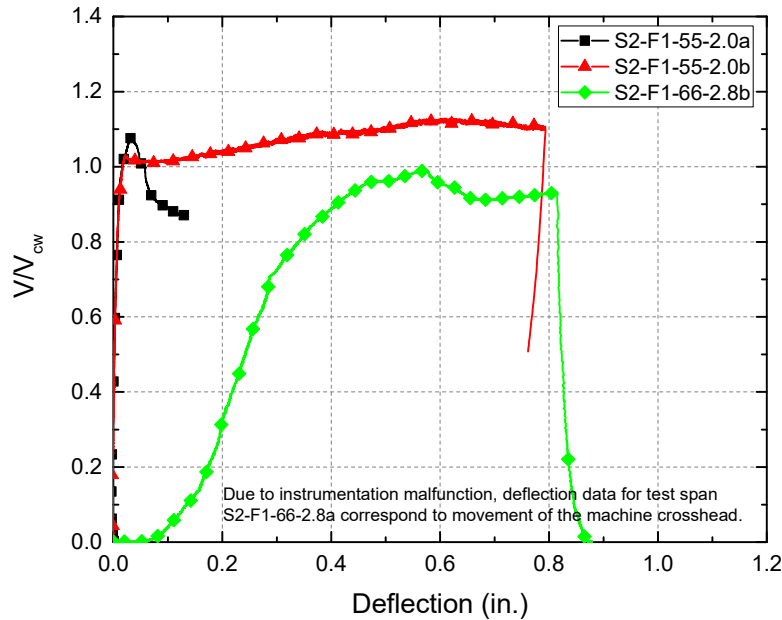

Figure 14 - Normalized shear versus deflection response for Series 2 test spans without external prestressing and L_{end} = 48.0 or 43.5 in. (1220 or 1105 mm)

Test shear spans with external prestressing

The remaining ten test shear spans were subjected to an external prestressing of 80 kips (360 kN) and had a distance between the center of the support and the slab edge of 1.75 in. (45 mm). The length of the shear spans for these tests ranged between 2.8 and 3.0 the effective depth d. Except for test span S2-F2-50-2.9, these shear spans exhibited consistent behavior (Fig. 15). As shown in Fig. 15, the behavior of these spans was characterized by a linear response up to the formation of a flexural crack at or near the loading point. Once flexural cracking occurred, the response was significantly more flexible, with a nearly linear shear versus deflection relationship up to the development of web-shear cracking in several of the interior webs near the support, which led to

25

a sudden loss of load carrying capacity (see Fig. 16 for a typical cracking pattern and Appendix B for photos of all test shear spans). For the case of test shear span S2-F2-40-3.0, web diagonal cracking was also observed on the outer webs. It should be mentioned that in a few cases, flexural cracks turned into flexural-shear cracks, but the failure crack was always a web diagonal crack. Peak shear force for these test shear spans, excluding span S2-F2-50-2.9, ranged between 0.89 and 1.21V_{cw} (see Table 2).
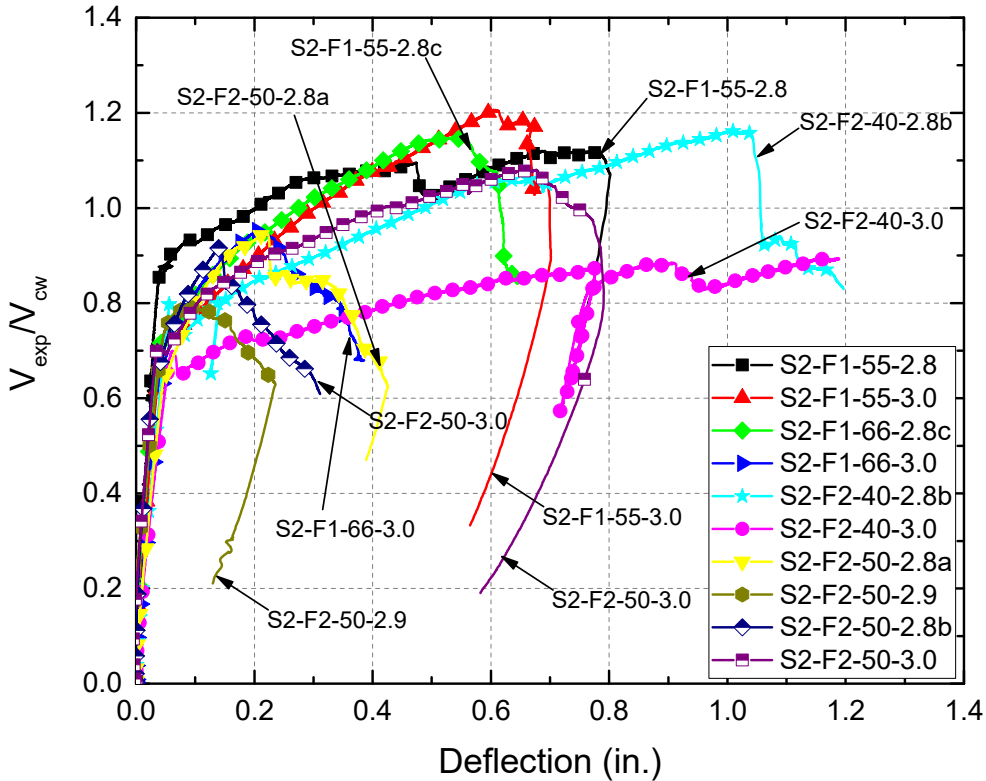
Figure 15 - Normalized shear force versus deflection response for Series 2 test spans with external prestressing

The exception in terms of behavior for the test shear spans with external prestressing was test span S2-F2-50-2.9. This shear span first exhibited flexural-shear cracking near the loading point at a shear force of 0.8V_{cw}. Upon the application of additional deflection, the load remained nearly constant, indicating the occurrence of strand slip. This was followed by web diagonal cracking

near the support, which is believed to have occurred due to a reduction in effective prestress as the strands slipped.

As mentioned earlier, it was not possible to test a slip-formed slab with regular concrete as part of this investigation. However, Palmer and Schultz (2010) reported on the tests of eight 16-in. (405-mm) deep slip-formed slabs with a shear span-to-effective depth ratio of approximately 2.5. Peak shear forces in those slabs ranged between 0.74 and $1.07V_{cw}$ for an average value of $0.88V_{cw}$. The slip-formed slabs tested in this investigation that failed in shear, on the other hand, exhibited peak shear forces ranging between 0.80 and $1.21V_{cw}$ for an average value of $1.04V_{cw}$. Further, the three spans reinforced with Type 1 fibers that failed in shear (all with fibers at 55 lbs/yd^3 or 320 N/m^3) for which transfer lengths were, on average, comparable to those reported by Palmer and Schultz (approximately $50d_b$), exhibited peak shear forces ranging between 1.08 and $1.21V_{cw}$. Assuming a comparison between the peak strengths of the slip-formed slabs tested in this investigation and those reported in Palmer and Schultz (2010), it does seem that fiber reinforcement led to an increase in shear strength, especially in the case of Type 1 fibers for which similar end slip values were measured. As shown in Fig. 10b, significantly larger strand end slips were measured for the slabs with Type 2 fibers, which would have somewhat offset the better behavior exhibited by the material beams with these fibers (Fig. 9b), and led to greater variability in web-cracking shear strength. The limited data suggest that slabs with Type 1 and Type 2 fibers in the dosages evaluated should lead to shear strengths of at least V_{cw}, as long as transfer lengths of approximately $50d_b$ or shorter can be achieved.

Figure 16 - Typical web cracking for test spans in Series 2 with external prestressing

3. CONCLUSIONS

Based on the results from the tests of several precast, prestressed concrete fiber reinforced concrete hollow-core slabs constructed following either an extrusion or a slip-form process, the following conclusions can be drawn.

- Extruded hollow-core slabs with Type 1 and Type 2 fibers in volume fractions of up to 0.38% (50 lbs/yd^3 or 290 N/m^3) could be mixed without any changes to the original mixture proportions or mixing process. Type 1 fibers were 1.18 in. (30 mm) long and 0.022 in. (0.55 mm) in diameter, while Type 2 fibers were 2.4 in. (60 mm) long and 0.035 in. (0.90 mm) in diameter. From observations during manufacturing of the slabs and the test results, it appears that some difficulties in terms of mixing and fiber distribution could be encountered when using Type 2 fibers in a 0.5% volume fraction.

- Manufacturing of slip-formed hollow-core slabs proved challenging when using Type 2 fibers, particularly in volume fractions of 0.38%. In some instances, manufacturing of these slabs had to be paused to clear fibers trapped in the slip-form machine. On the other hand, no major difficulties were encountered in the manufacturing of slabs with Type 1 fibers at dosages of up to 0.5% by volume. It is thus recommended that until more information become available, fibers used in the manufacturing of slip-formed hollow-core slabs should not be longer than 1.2 in. (30 mm) and in volume fractions not greater than 0.5%.

- Strand end slip values in the slabs constructed using an extrusion method did not seem to be affected by the presence of fibers. Fifty strand diameters ($50d_b$) represented an adequate, and generally conservative estimation of the average transfer length for the 0.6 in. diameter strands, and was in all cases conservative for estimating transfer length for the 0.5 in. diameter strands. Measured slip values for the slabs manufactured using a slip-form process, on the other hand, showed a much greater variability compared to the measured slips in the extruded slabs. Measured slips were smallest for the strands in the slabs with Type 1 fibers at a 0.42% volume fraction (55 lbs/yd^3 or 320 N/m^3), with most values near or below that corresponding to a transfer length of 50 strand diameters. The strands in the slabs with Type 1 fibers at a 0.5% volume fraction (66 lbs/yd^3 or 385 N/m^3) showed a similar trend, but with larger slip values that in most cases exceeded that

29

corresponding to a transfer length of $50d_b$. Measured slip values for the slabs with Type 2 fibers at a 0.38% volume fraction (50 lbs/yd^3 or 290 N/m^3), on the other hand, were significantly greater than those in the slabs with Type 1 fibers, exceeding in most cases $80d_b$. This is believed to have been caused by the difficulties encountered in the manufacturing of the slabs with these fibers, which were twice as long as the Type 1 fibers.

- Extruded fiber-reinforced concrete slabs with Type 1 and Type 2 fibers at a 0.38% and 0.30% volume fraction, respectively, exhibited peak shear strengths that ranged between 1.08 and 1.20 times the calculated web-cracking shear strength, V_{cw}. The two extruded slabs without fibers, on the other hand, failed at shear forces corresponding to 0.93 and 0.87 times the calculated web-cracking shear strength. The extruded slabs with Type 2 fibers at 0.38% and 0.50% volume fraction showed a greater variability in shear strength, likely due to variations in fiber distribution or concrete compaction. These slabs failed at shear strengths ranging between 0.94 and 1.29 times the calculated web-cracking shear strength. Besides an increase in shear strength, the presence of fibers, particularly of Type 2 fibers, led to a more gradual post-peak strength decay.

- Several of the slip-formed slabs exhibited a behavior governed by strand slip after flexural cracking. This led to the use of external prestressing as a means to increase flexural strength and induce a shear failure. The test slip-formed slabs that failed in shear exhibited peak shear forces ranging between 0.80 and $1.21V_{cw}$ for an average value of $1.04V_{cw}$. The three spans reinforced with Type 1 fibers that failed in shear (all with fibers at 55 lbs/yd^3 or 320 N/m^3) for which transfer lengths were, on average, approximately $50d_b$, exhibited peak shear forces ranging between 1.08 and $1.21V_{cw}$. A greater variability of shear strength was observed in the slabs with Type 2 fibers, for which significantly larger transfer lengths were calculated.

- Even though no regular concrete slip-formed slab was tested as part of this investigation, a comparison of the shear strength of the spans that exhibited a web-cracking shear failure with that of eight slip-formed slabs tested by Palmer and Schultz (2010) suggests that the use of fiber reinforcement leads to an increase in shear strength, especially when considering the slabs with Type 1 fibers for which similar transfer lengths were calculated. The limited data suggest that slabs with Type 1 and Type 2 fibers in the

dosages evaluated should lead to shear strengths of at least V_{cw}, as long as transfer lengths of approximately $50d_b$ or shorter can be achieved.

4. REFERENCES

American Society for Testing Materials, ASTM (2012). *Standard Test Method for Flexural Performance of Fiber-Reinforced Concrete (Using Beam With Third-Point Loading)*, ASTM C 1609/C 1609M-12, West Conshohocken, PA, ASTM International.

Chao, S.-H., Naaman, A. E., and Parra-Montesinos, G. J. (2009). "Bond Behavior of Reinforcing Bars in Tensile Strain-hardening Fiber-Reinforced Cement Composites," *ACI Structural Journal*, V. 106, No. 6, pp. 897-906.

Cuenca, E., and Serna, P. (2013). "Failure Modes and Shear Design of Prestressed Hollow Core Slabs Made of Fiber-Reinforced Concrete*," Composites: Part B,* Elsevier, V. 45, pp. 952-964.

Dinh, H. H., Parra-Montesinos, G. J., and Wight, J.K. (2010). "Shear Behavior of Steel Fiber-Reinforced Concrete Beams without Stirrup Reinforcement," *ACI Structural Journal*, V. 107, No. 5, pp. 597-606.

Dudnik V.S., Milliman, L.R., and Parra-Montesinos, G.J. (2017). "Shear Behavior of Prestressed Steel Fiber Reinforced Concrete Hollow-Core Slabs," *PCI Journal*, July-August 2017, pp. 58-72.

Hawkins, N. M., and Ghosh, S. (2006). "Shear Strength of Hollow-Core Slabs," *PCI Journal,* V.51, No. 1, pp. 110-115.

Northern Digital Inc. (2011). *NDI OptoTRAK Certus User Guide*, Waterloo, ON, Canada.

Palmer, K. D., and Schultz, A. E. (2010). "Web Shear Strength of Precast, Prestressed Concrete Hollow Core Slab Units," Department of Civil Enginering, University of Minnesota, January 2010m 270 pp.

Parra-Montesinos, G. J. (2006). "Shear Strength of Beams with Deformed Steel Fibers," *Concrete International*, V. 28, No. 11, pp. 61-70.

APPENDIX A – NORMALIZED SHEAR FORCE VERSUS DEFLECTION RESPONSE FOR TEST SPANS
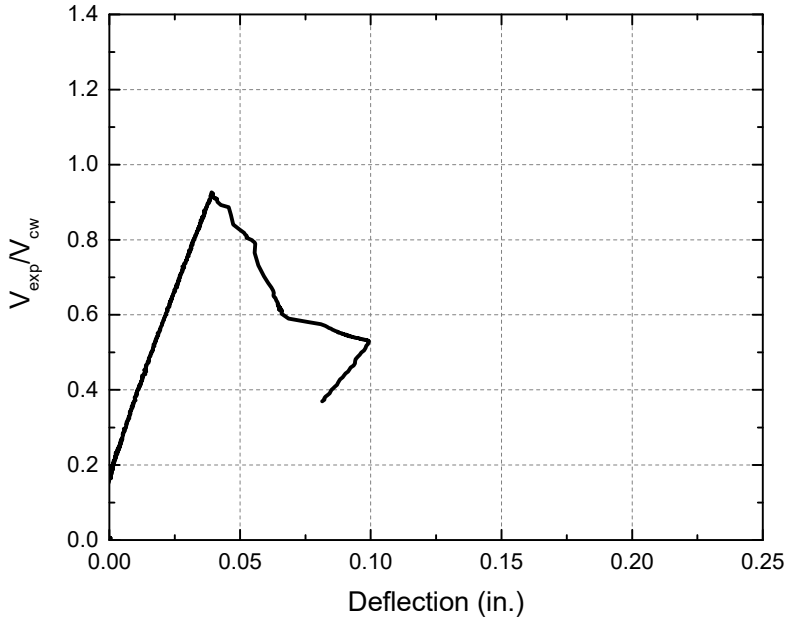
Figure A1 - Normalized shear force versus deflection response for test span S1-NF-3.0
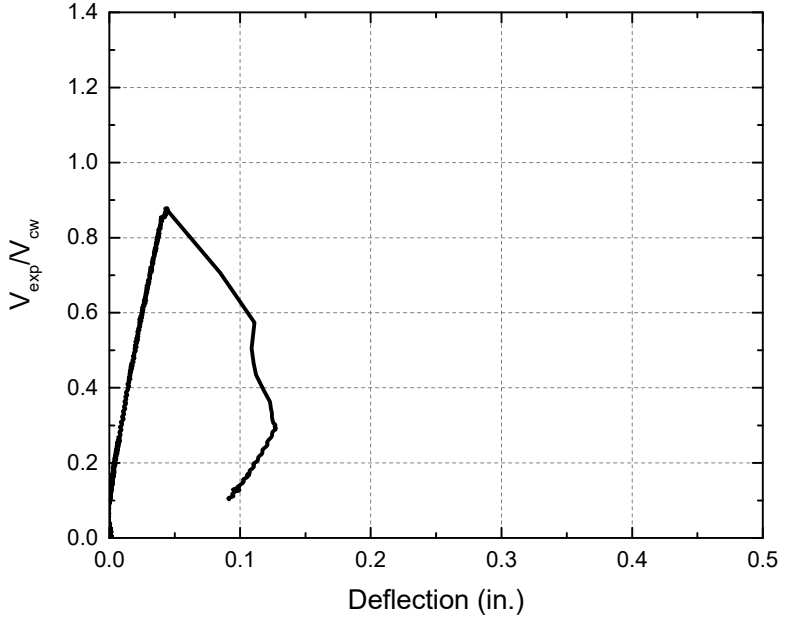
**Figure A2 - Normalized shear force versus deflection response for test span S1-NF-3.5**
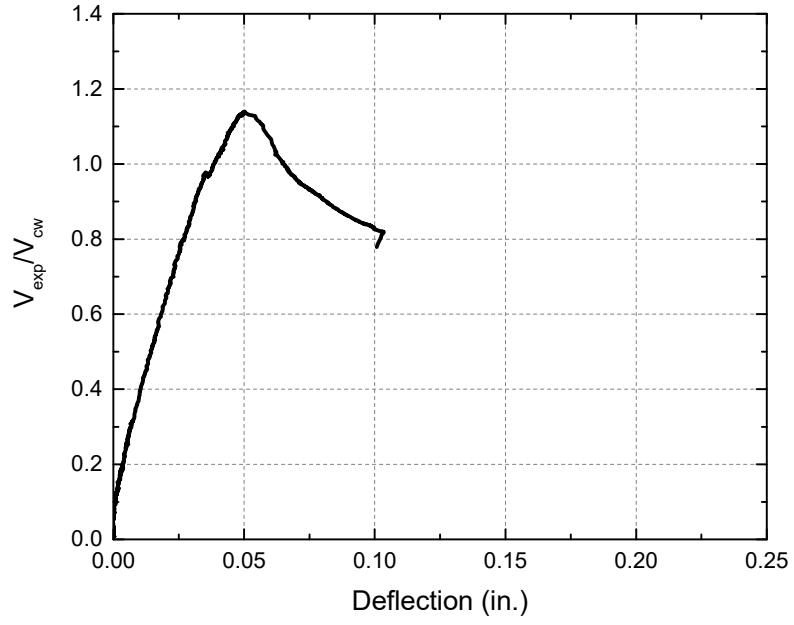
**Figure A3 - Normalized shear force versus deflection response for test span S1-F1-50-3.0**
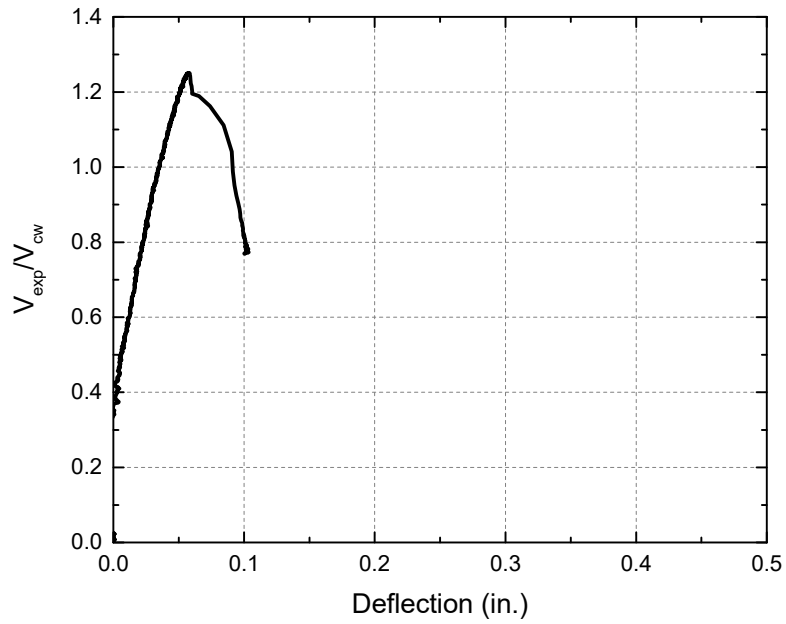
Figure A4 - Normalized shear force versus deflection response for test span S1-F1-50-3.5
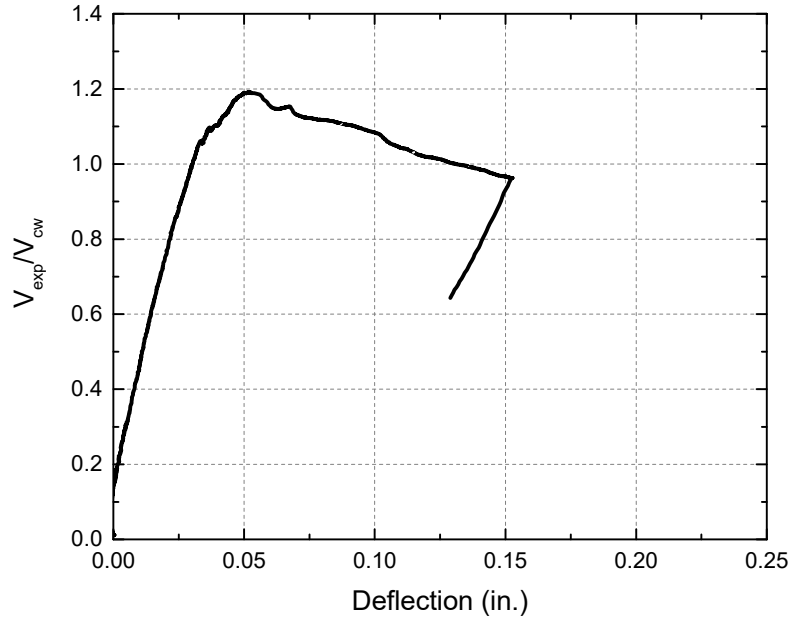
Figure A5 - Normalized shear force versus deflection response for test span S1-F2-40-3.0a
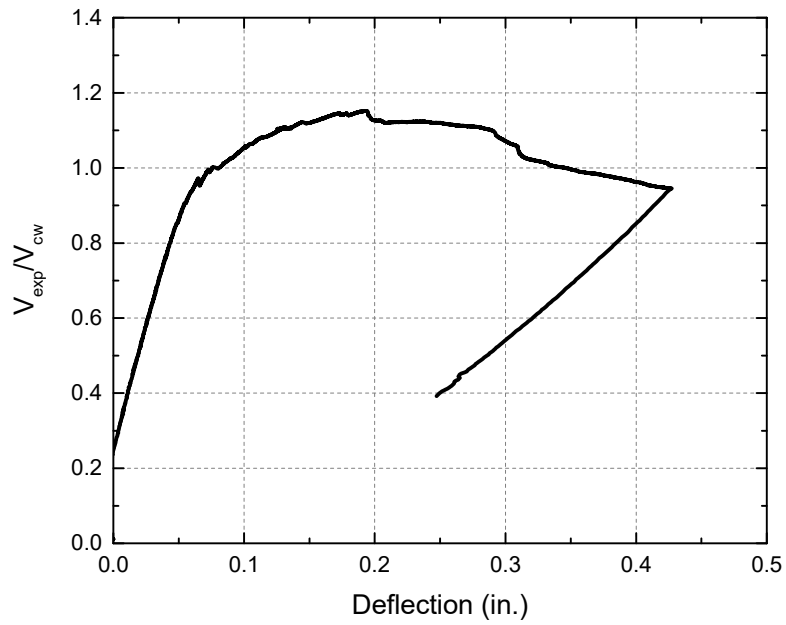

Figure A6 - Normalized shear force versus deflection response for test span S1-F2-40-3.5a
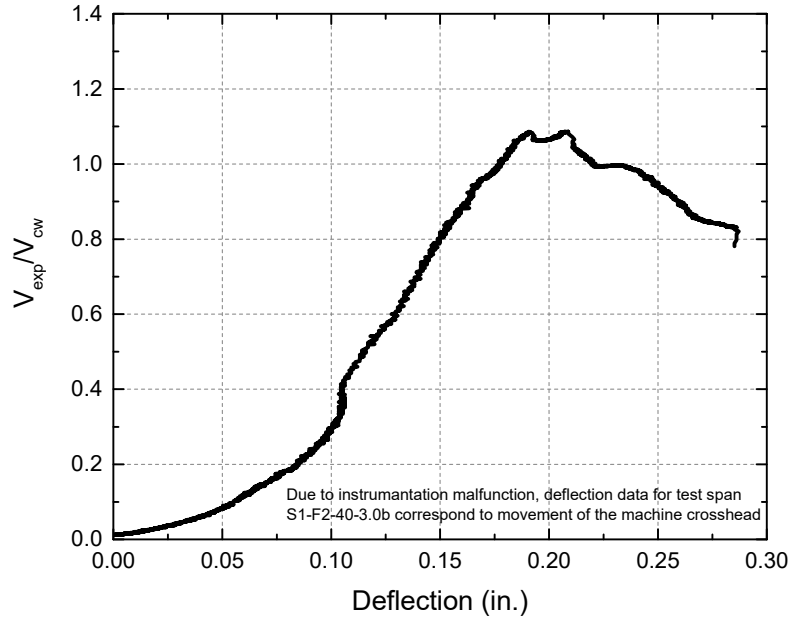
Figure A7 - Normalized shear force versus deflection response for test span S1-F2-40-3.0b
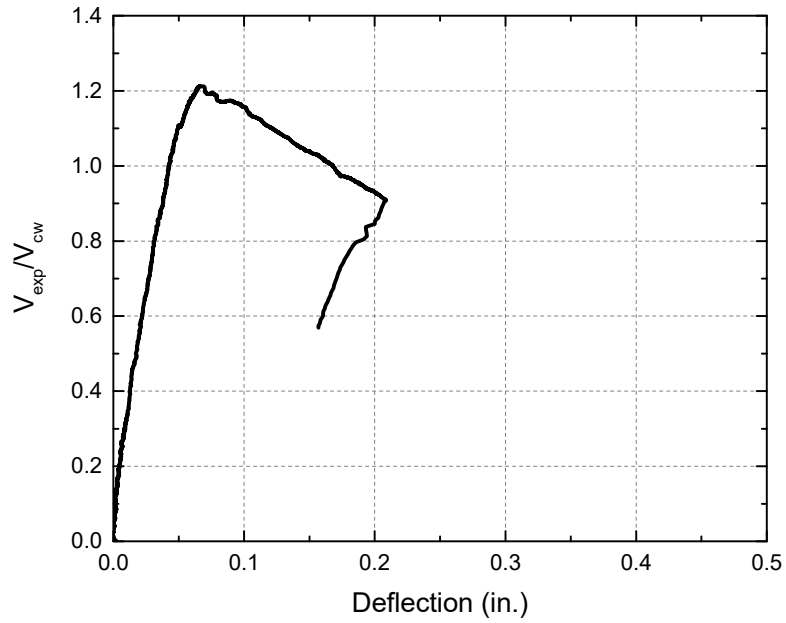
Figure A8 - Normalized shear force versus deflection response for test span S1-F2-40-3.5b

36
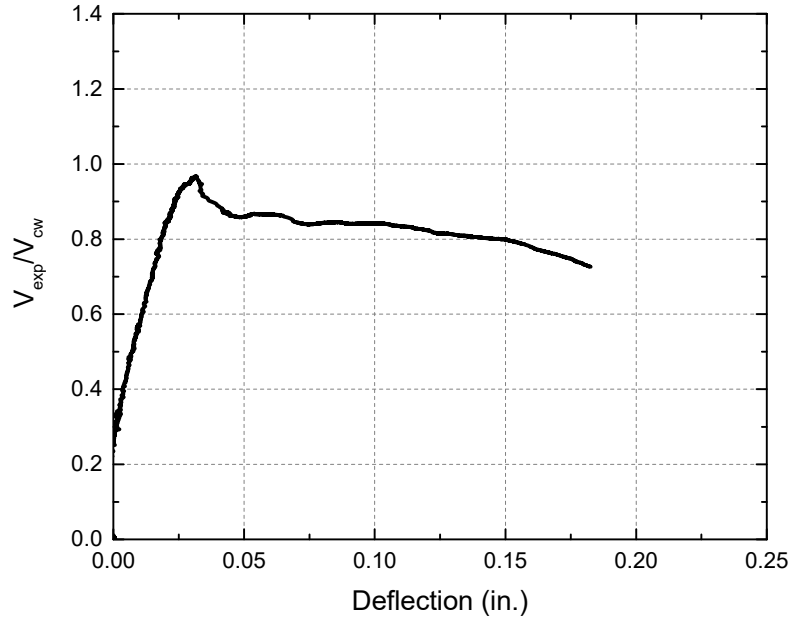
Figure A9 - Normalized shear force versus deflection response for test span S1-F2-50-3.0a
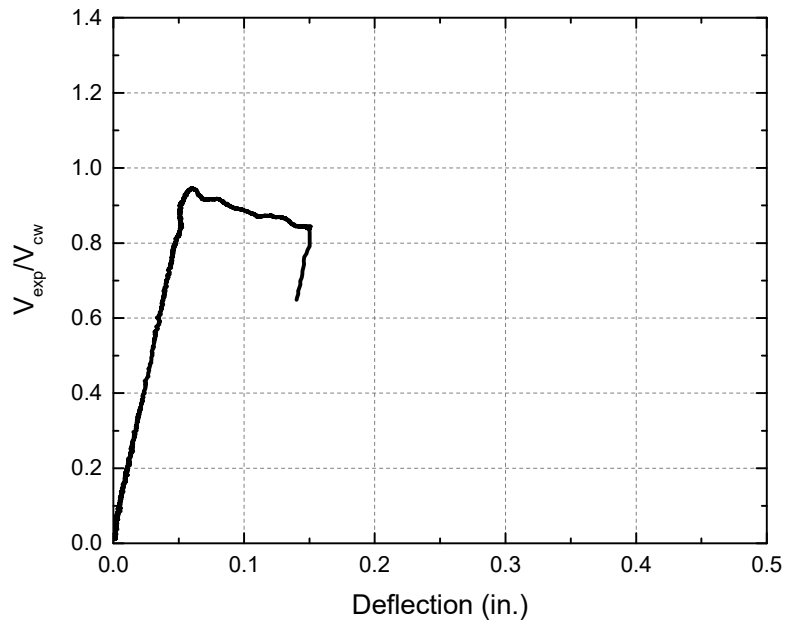
**Figure A10 - Normalized shear force versus deflection response for test span S1-F2-50-3.5a**
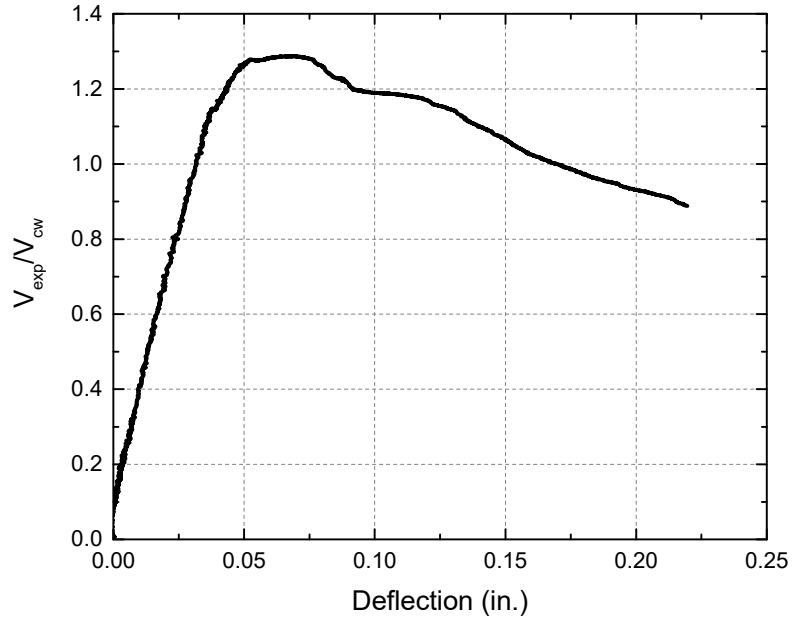
Figure A11 - Normalized shear force versus deflection response for test span S1-F2-50-3.0b
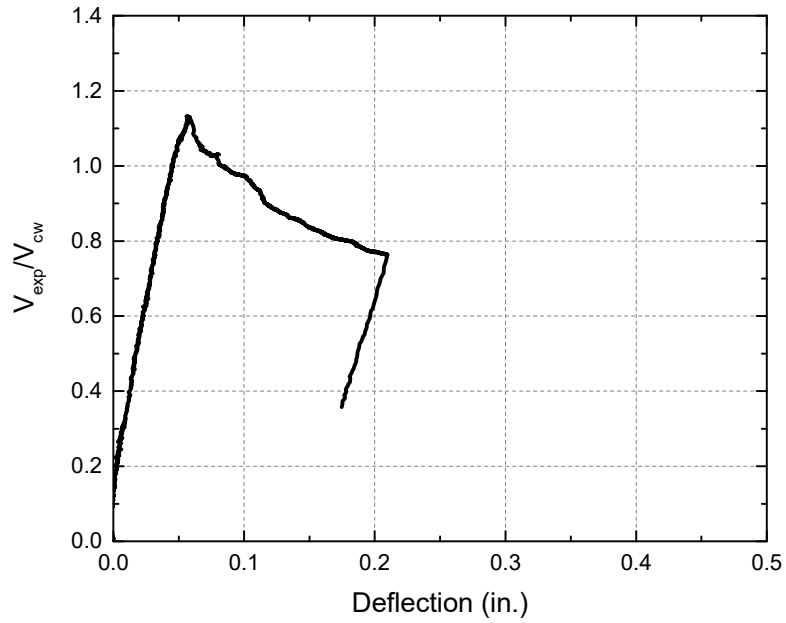
Figure A12 - Normalized shear force versus deflection response for test span S1-F2-50-3.5b
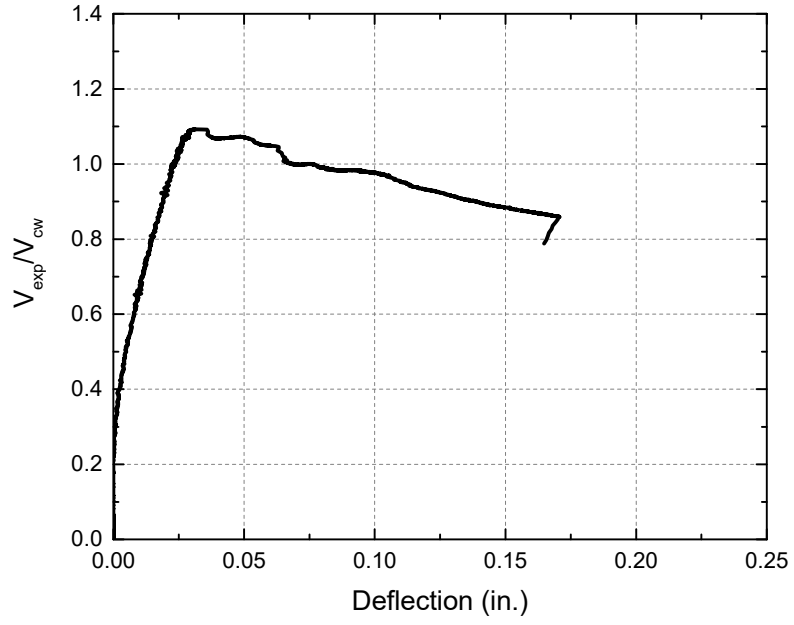
Figure A13 - Normalized shear force versus deflection response for test span S1-F2-62-3.0
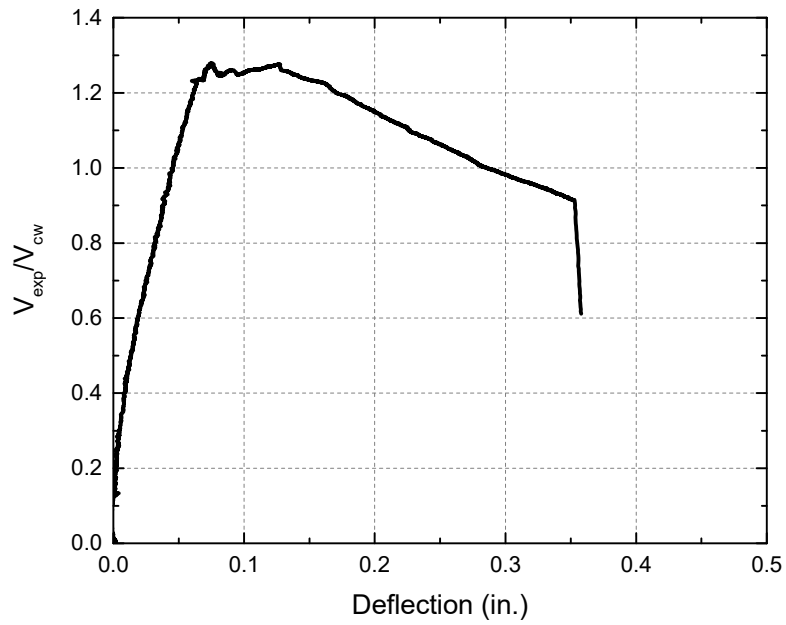
Figure A14 - Normalized shear force versus deflection response for test span S1-F2-62-3.5
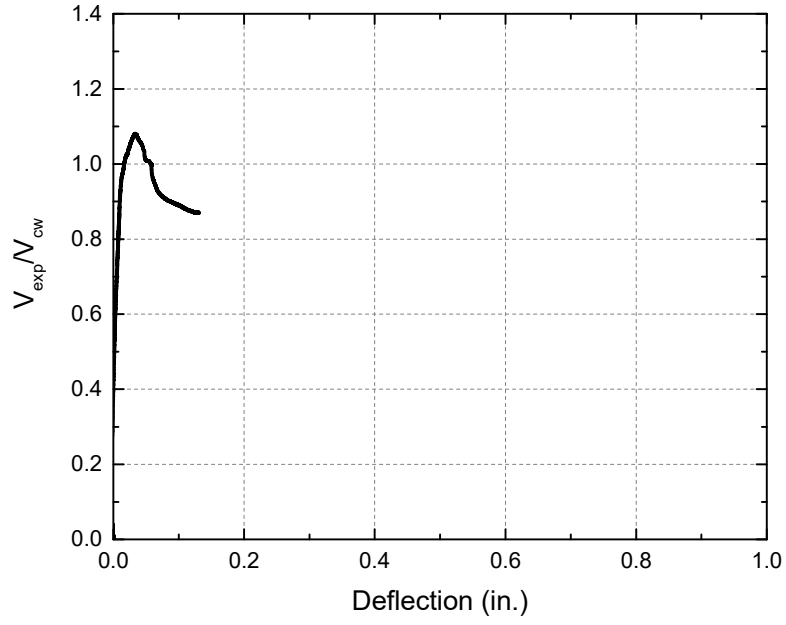
Figure A15 - Normalized shear force versus deflection response for test span S2-F1-55-2.0a
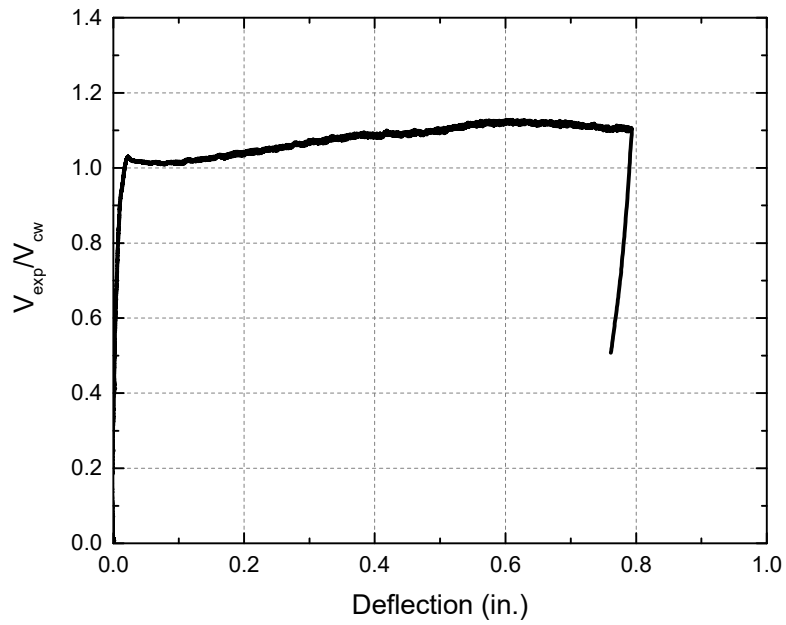
**Figure A16 - Normalized shear force versus deflection response for test span S2-F1-55-2.0b**
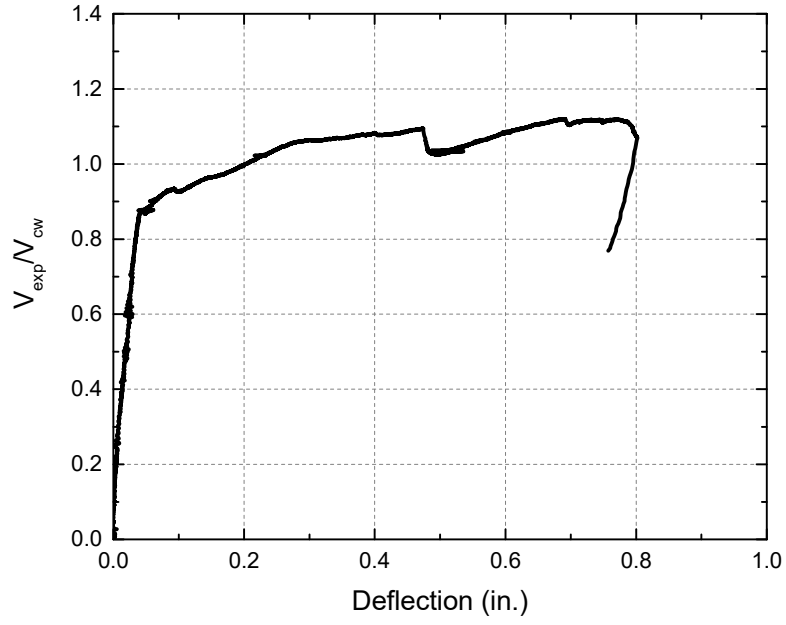
**Figure A17 - Normalized shear force versus deflection response for test span S2-F1-55-2.8**
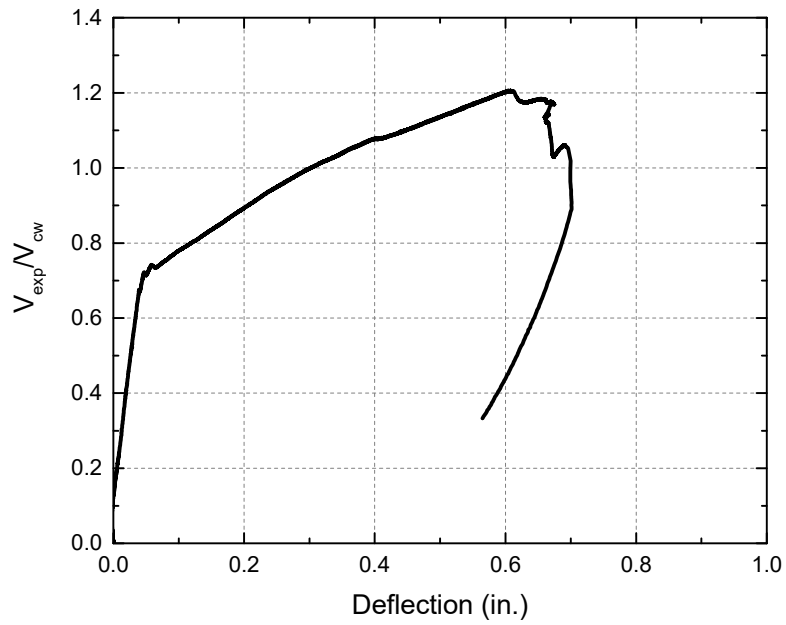
Figure A18 - Normalized shear force versus deflection response for test span S2-F1-55-3.0
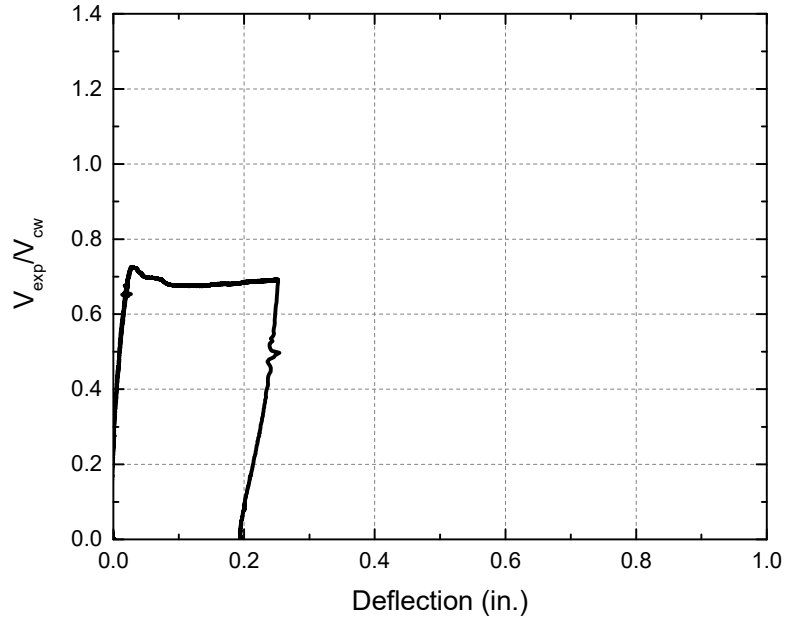
Figure A19 - Normalized shear force versus deflection response for test span S2-F1-66-2.3
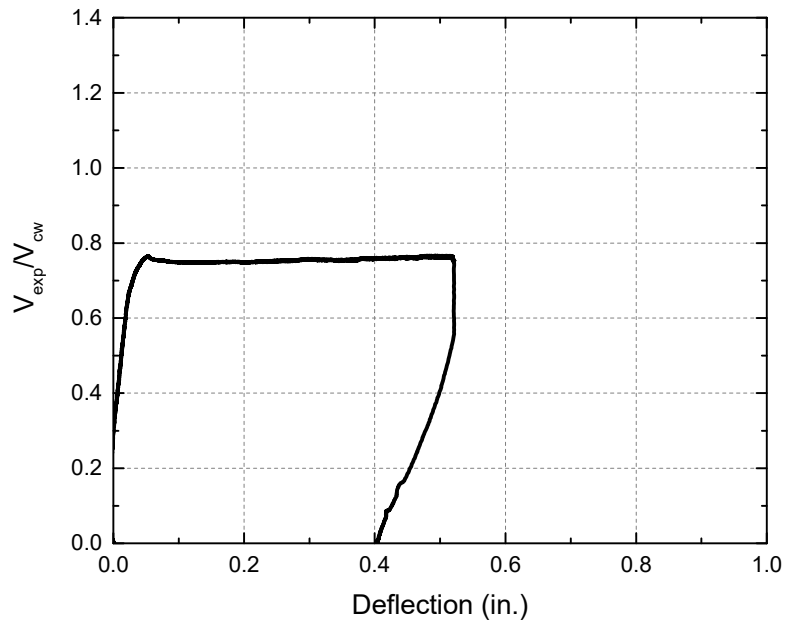
**Figure A20 - Normalized shear force versus deflection response for test span S2-F1-66-2.8a**

Due to instrumentation malfunction, deflection data for test span S2-F1-66-2.8a correspond to movement of the machine crosshead.
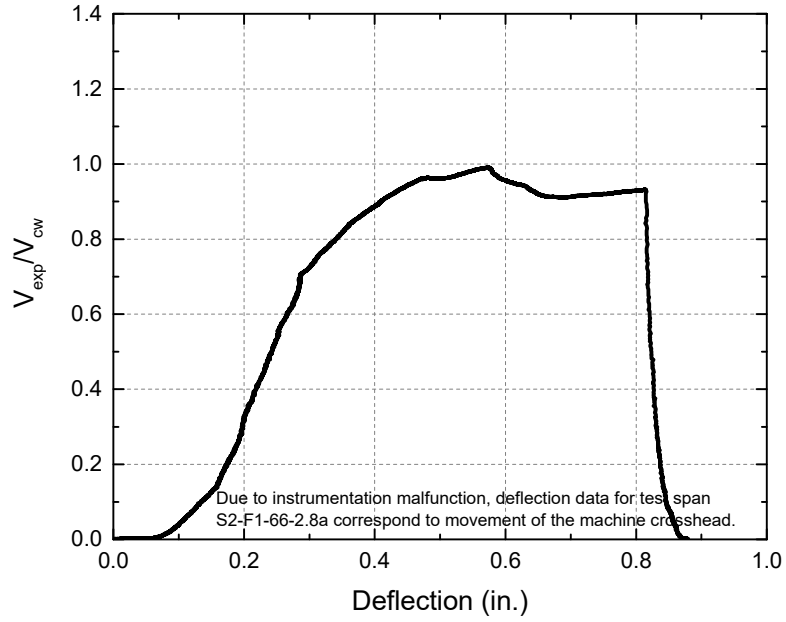
Figure A21 - Normalized shear force versus deflection response for test span S2-F1-66-2.8b
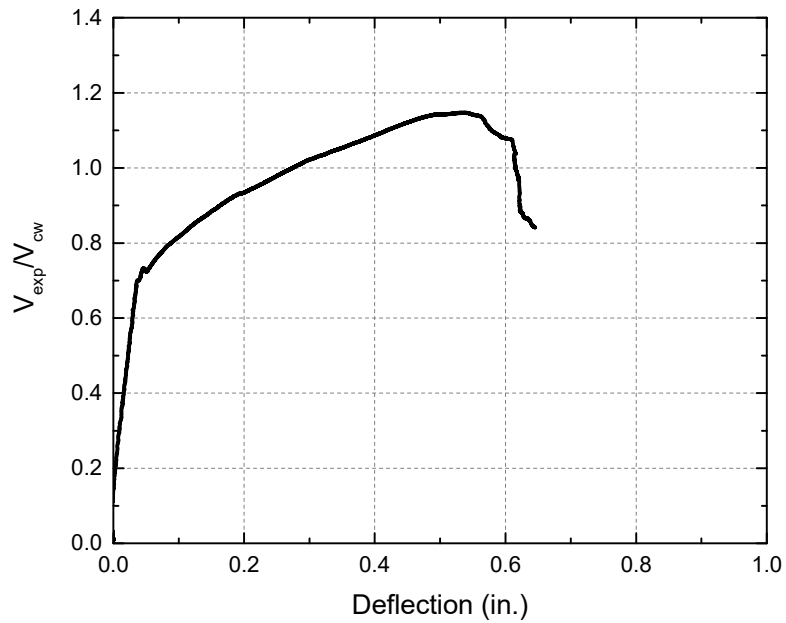
Figure A22 - Normalized shear force versus deflection response for test span S2-F1-66-2.8c
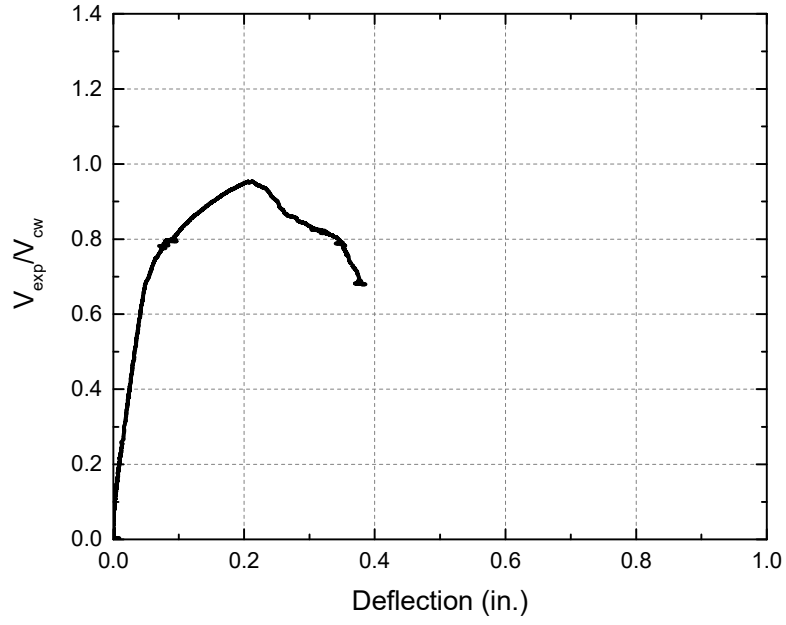
Figure A23 - Normalized shear force versus deflection response for test span S2-F1-66-3.0
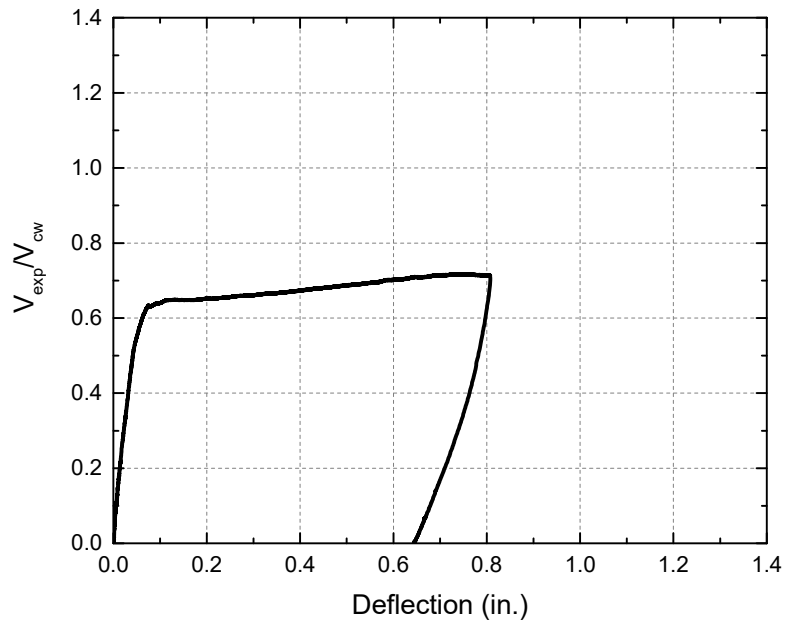
Figure A24 - Normalized shear force versus deflection response for test span S2-F2-40-2.8a
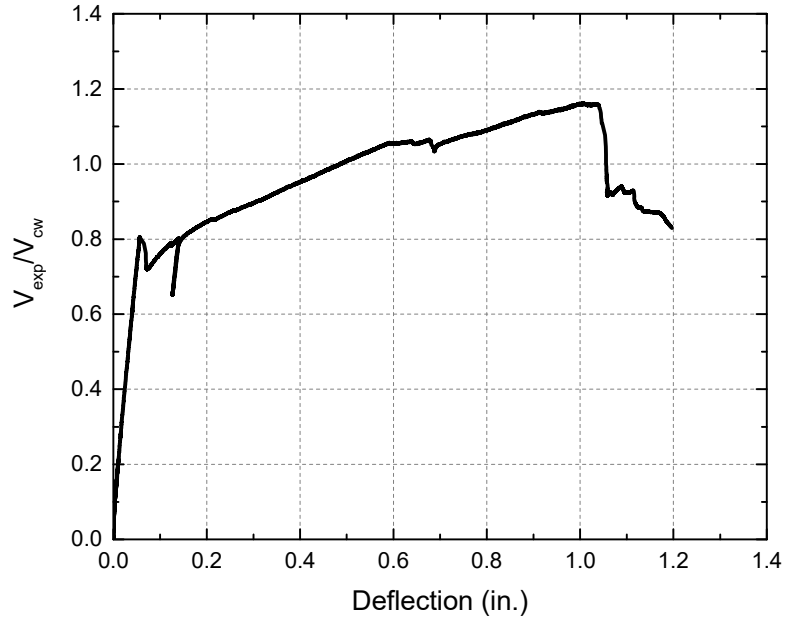
**Figure A25 - Normalized shear force versus deflection response for test span S2-F2-40-2.8b**
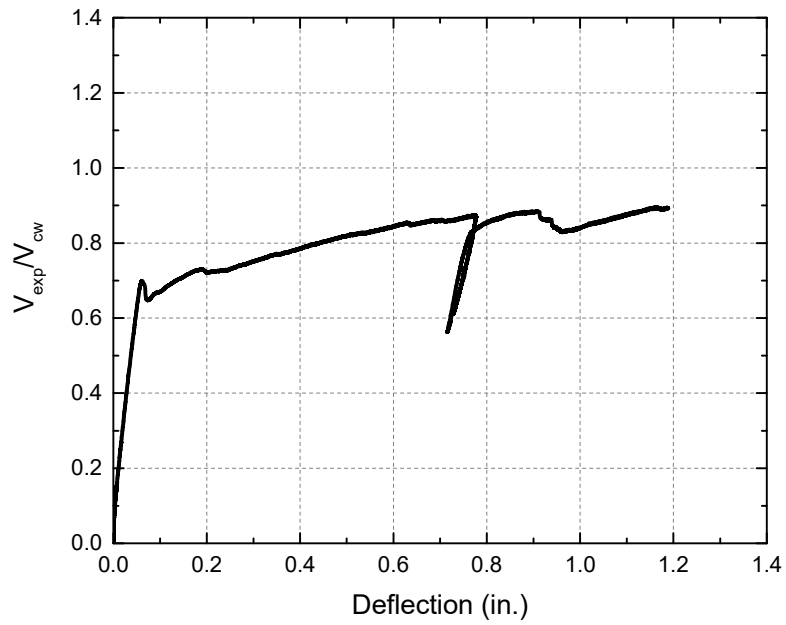
**Figure A26 - Normalized shear force versus deflection response for test span S2-F2-40-3.0**
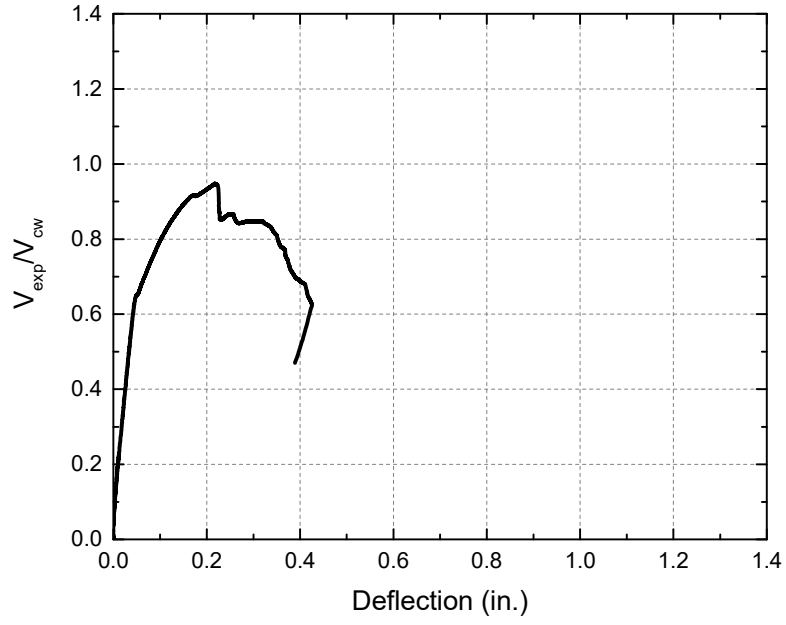
Figure A27 - Normalized shear force versus deflection response for test span S2-F2-50-2.8a
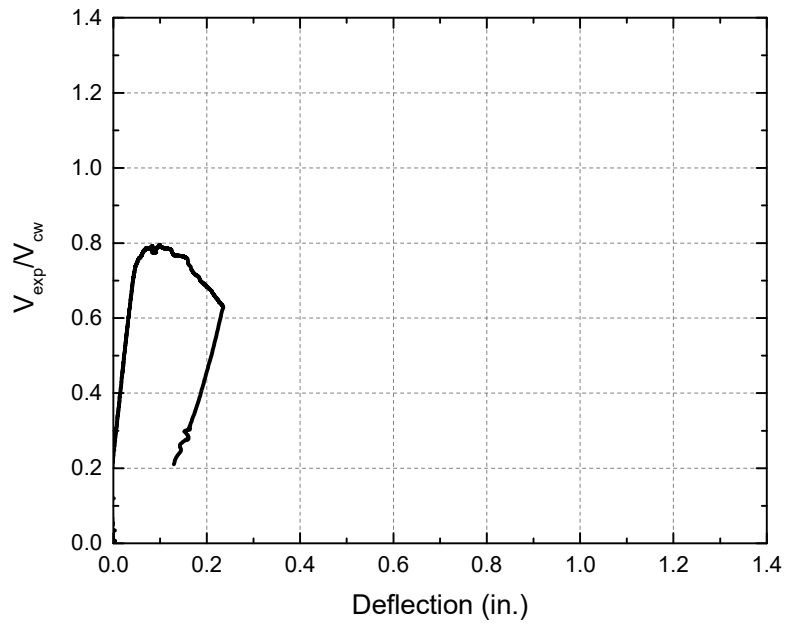

**Figure A28 - Normalized shear force versus deflection response for test span S2-F2-50-2.9**
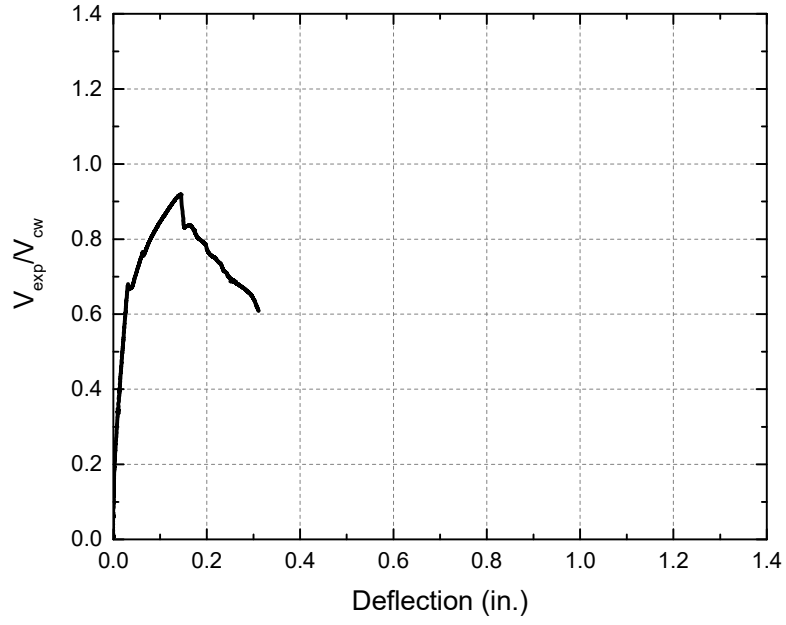
Figure A29 - Normalized shear force versus deflection response for test span S2-F2-50-2.8b
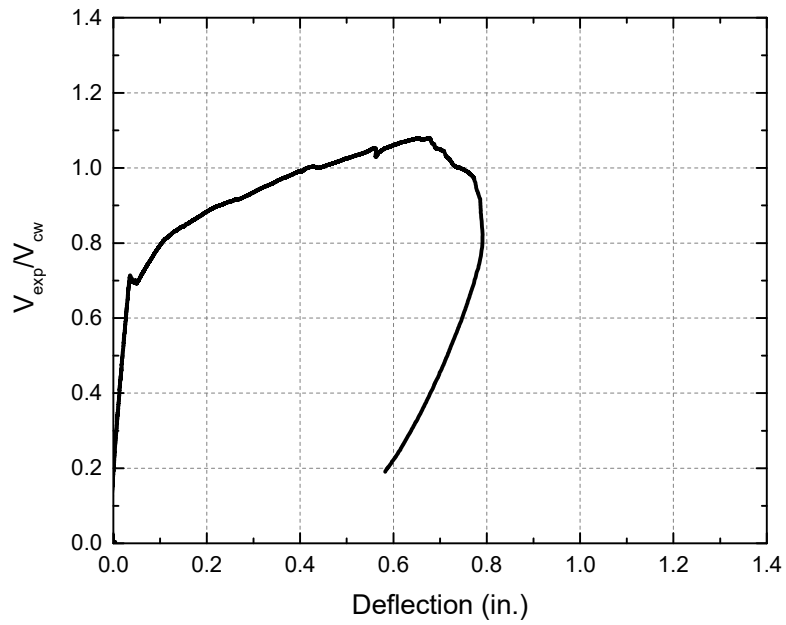

Figure A30 - Normalized shear force versus deflection response for test span S2-F2-50-3.0

47

APPENDIX B – PHOTOS OF TEST SPANS

Figure B1 - Test span S1-NF-3.0

Figure B2 - Test span S1-NF-3.5

Figure B3 - Test span S1-F1-50-3.0

Figure B4 - Test span S1-F1-50-3.5

Figure B5 - Test span S1-F2-40-3.0a

Figure B6 - Test span S1-F2-40-3.5a

Figure B7 - Test span S1-F2-40-3.0b

Figure B8 - Test span S1-F2-40-3.5b

51

Figure B9 - Test span S1-F2-50-3.0a

Figure B10 - Test span S1-F2-50-3.5a

Figure B11 - Test span S1-F2-50-3.0b

Figure B12 - Test span S1-F2-50-3.5b

Figure B13 - Test span S1-F2-62-3.0

Figure B14 - Test span S1-F2-62-3.5

Figure B15 - Test span S2-F1-55-2.0a
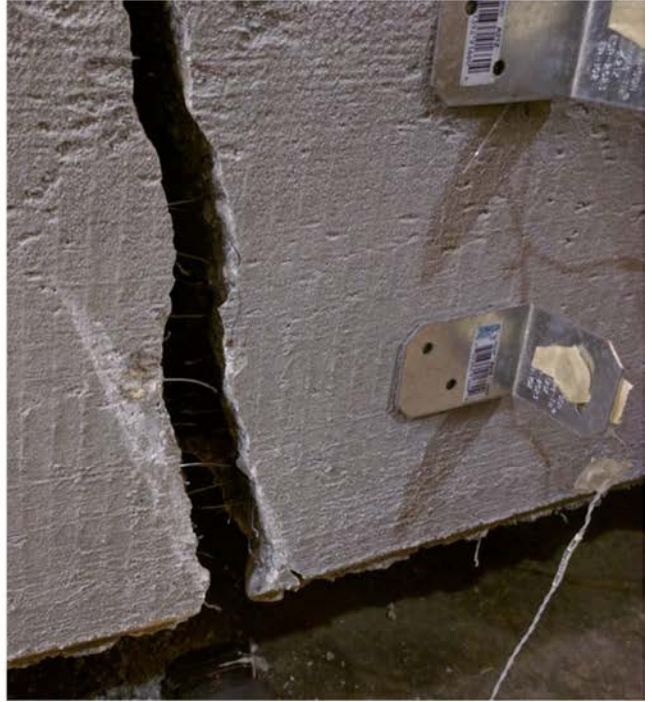
Figure B16 - Test span S2-F1-55-2.0b

Figure B17 - Test span S2-F1-55-2.8

Figure B18 - Test span S2-F1-55-3.0

Figure B19 - Test span S2-F1-66-2.3

Figure B20 - Test span S2-F1-66-2.8a

Figure B21 - Test span S2-F1-66-2.8b

Figure B22 - Test span S2-F1-66-2.8c

Figure B23 - Test span S2-F1-66-3.0

Figure B24 - Test span S2-F2-40-2.8a

Figure B25 - Test span S2-F2-40-2.8b

Figure B26 - Test span S2-F2-40-3.0
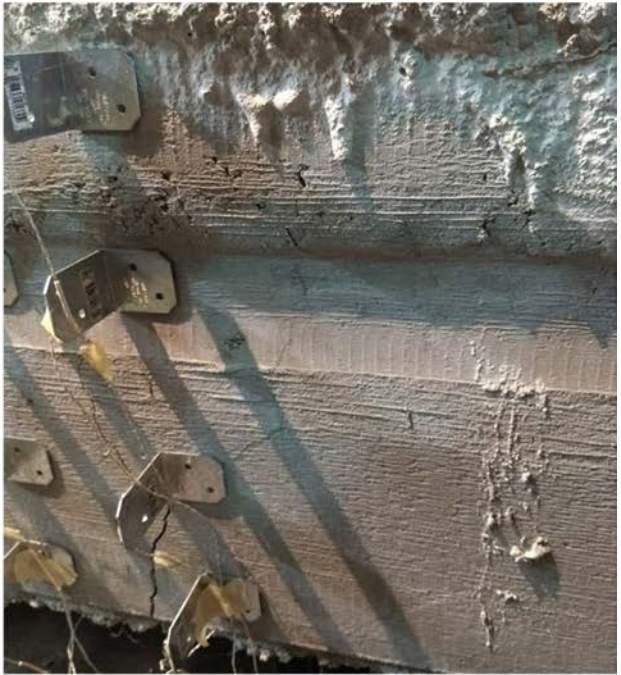
Figure B27 - Test span S2-F2-50-2.8a

Figure B28 - Test span S2-F2-50-2.9

Figure B29 - Test span S2-F2-50-2.8b

Figure B30 - Test span S2-F2-50-3.0